Tectonophysics 586 (2013) 15–34

Contents lists available at SciVerse ScienceDirect

Tectonophysics

journal homepage: www.elsevier.com/locate/tecto

Review Article

A review of the 2011 Tohoku-Oki earthquake (Mw 9.0): Large-scale rupture across heterogeneous plate coupling

Fumiko Tajima [a,*], Jim Mori [b], Brian L.N. Kennett [c]

[a] Depart. Earth and Environ. Sci., Ludwig-Maximilians-University (LMU), München, Theresienstr. 41, 80333 München, Germany
[b] Disaster Prevention Research Institute (DPRI), Kyoto University, Uji, Kyoto, 611, Japan
[c] Research School of Earth Sciences, The Australian National University, Canberra, ACT 0200, Australia

ARTICLE INFO

Article history:
Received 5 May 2012
Received in revised form 1 September 2012
Accepted 8 September 2012
Available online 24 September 2012

Keywords:
2011 Mw 9 Tohoku-Oki megathrust earthquake
Separation of source areas of high- and low-frequency radiations
Large slip near the trench
Interlocking of heterogeneous plate coupling
Variations of physical properties revealed in tomographic images

ABSTRACT

The 2011 Tohoku-Oki earthquake ruptured a large source region, which included areas with a range of past M 7 to M 8 earthquakes, varying stress accumulation, and different structural features. This megathrust event was substantially larger than anticipated in this region, though there were indications that the sequences of events in recent times were insufficient to relieve the full accumulated strain in the relatively rapid subduction of the Pacific plate. The source process time of about 150 s included rupture of an area of very large slip (30 to 60 m) on the shallow portion of the megathrust, updip of the hypocenter. The area of large slip produced large amplitude low-frequency radiation, while the dominant high-frequency radiation was generated from deeper sources down-dip of the hypocenter. Real-time information systems in Japan were able to issue timely warnings of the strong shaking and tsunami, but the complicated pattern of rupture growth led to an underestimate in the initial estimates of magnitude and tsunami threat. Variations in the plate coupling and heterogeneities of physical properties in the megathrust zone characterize the different source areas that ruptured together during the earthquake. Tomographic images of shear-wave and bulk-sound speeds show subtle changes of physical properties that may be associated with coupling condition and present clues for understanding the rupture process of this Mw 9 earthquake, which combined the source areas of many past earthquakes.

Contents

1. Introduction . . . 16
2. Characterizations of large earthquakes prior to the 2011 Tohoku-Oki earthquake . . . 17
   2.1. Historical large earthquakes . . . 17
   2.2. Large earthquakes over the last century . . . 18
   2.3. Aftershock activity of past large earthquakes and repeating small events . . . 18
3. Characteristics of the mainshock and aftershock activity . . . 20
   3.1. Real-time information . . . 20
   3.2. Slip distribution models . . . 21
   3.3. Crustal stress accumulation and release . . . 22
   3.4. Similarity to tsunami earthquakes . . . 24
   3.5. Foreshock and aftershock patterns and triggered events . . . 25
4. Structural influences . . . 26
   4.1. Presence of heterogeneity in the subducting plate . . . 27
   4.2. Influence of heterogeneity on partitioning of rupture style . . . 28
   4.3. Stress transfer in heterogeneous structure . . . 29
5. Discussion and conclusions . . . 30

* Corresponding author. Tel.: +1 562 343 4148.
E-mail address: tajima@geophysik.uni-muenchen.de (F. Tajima).

0040-1951/$ – see front matter © 2012 Elsevier B.V. All rights reserved.
http://dx.doi.org/10.1016/j.tecto.2012.09.014

Acknowledgments . . . 32
References . . . 32

1. Introduction

The 2011 March 11 off the Pacific coast of Tohoku Earthquake with moment magnitude Mw 9.0 took place off the coast of northeastern Japan at 14:46:18.1, Japan Standard Time (JST). This megathrust earthquake, hereafter referred to as the 2011 Tohoku-Oki earthquake, is one of the largest seismic events recorded by modern instruments, and is comparable to the 1960 Chile (Mw 9.5), the 1964 Alaska (Mw 9.2) and the 2004 Sumatra–Andaman (Mw = 9.0–9.3) earthquakes. The two recent great earthquakes have been the subject of extensive discussion about their mechanisms and variable nature of earthquake size within the same subduction zones and the relation to heterogeneous plate coupling. Over the last few decades, seismologists have developed models to characterize the rupture of large shallow subduction zone earthquakes in the context of plate coupling strength (Lay and Kanamori, 1981; Lay et al., 1982; Ruff and Kanamori, 1980, 1983). The 2011 Tohoku-Oki earthquake sequence ruptured a large portion of the boundary between the Pacific and the Okhotsk plates off the coast of the Tohoku region, Japan.

A systematic study that examined historic and recent seismicity data presented a hypothesis on the correlation between intraplate seismicity and large interplate earthquakes, and suggested the possibility of a large interplate event off the southern Sanriku in the near future (Seno, 1979). However, it has not yet been clarified if this region of the subduction zone was accumulating stress in a strongly coupled state or slipping more aseismically in a weakly coupled state. (e.g., Kanamori, 1977; Loveless and Meade, 2010; Seno and Eguchi, 1983; Tajima and Kanamori, 1985a, 1985b).

The Earthquake Research Committee (ERC) in Japan studied the probabilities for large subduction earthquakes based on over 400 years of historical records that included 24 M 7 and 6 M 8 class events in this region (Figs. 1 and 2), and gave probabilistic evaluations for various M 7 to M 8 earthquakes in the region (see Headquarters for Earthquake Research Promotion, http://www.jishin.go.jp/main/index-e.html and http://cais.

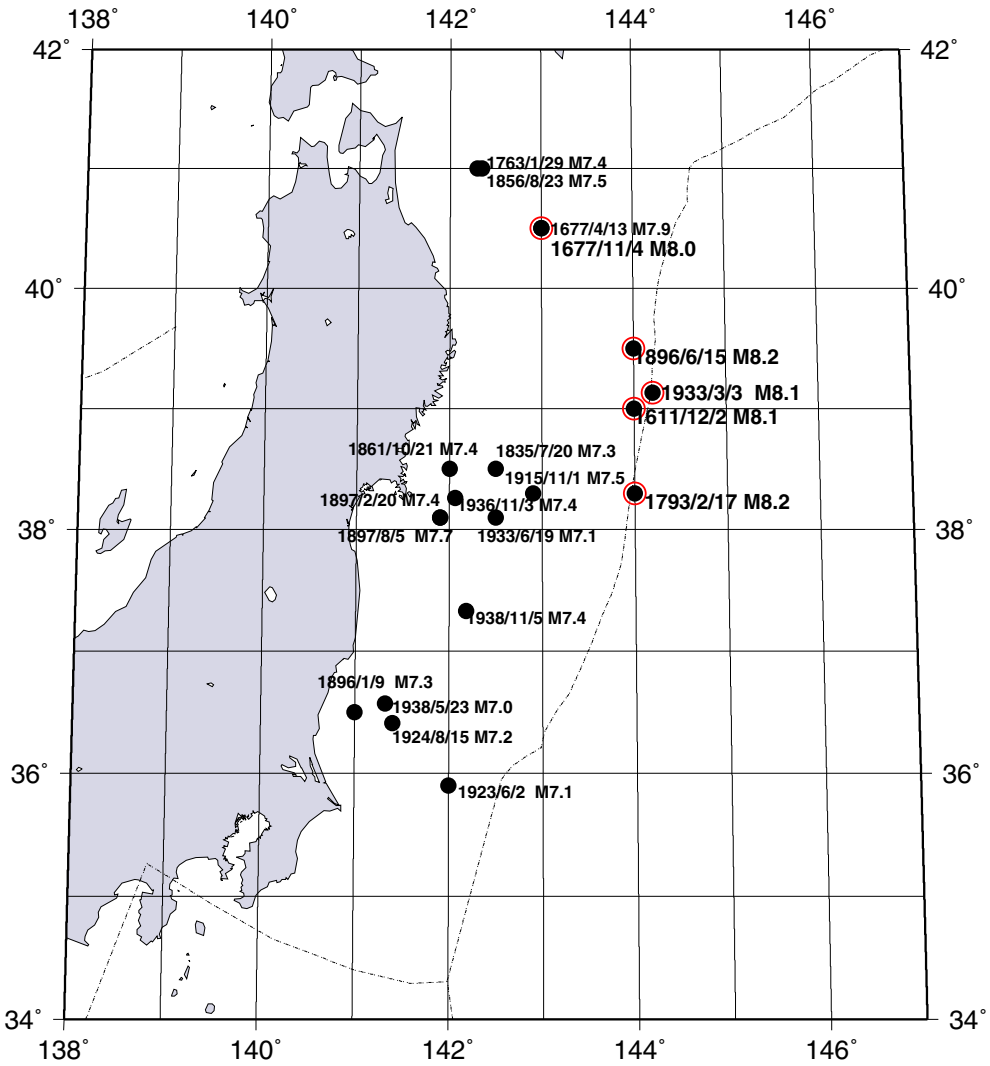

Fig. 1. Estimated epicenters (solid black circles) of historical earthquakes with M ≥7 (after Usami (1975) for events before 1800 and Utsu (2004); see the historical event catalogs at http://www.zisin.jp/modules/pico/index.php?cat_id=100). Events with M ≥8 are indicated by red open circles. Note that the historical event locations (or rupture areas) and magnitude estimates can vary among catalogs and study sources (e.g., the location of the 1793 earthquake in Seno, 1979).

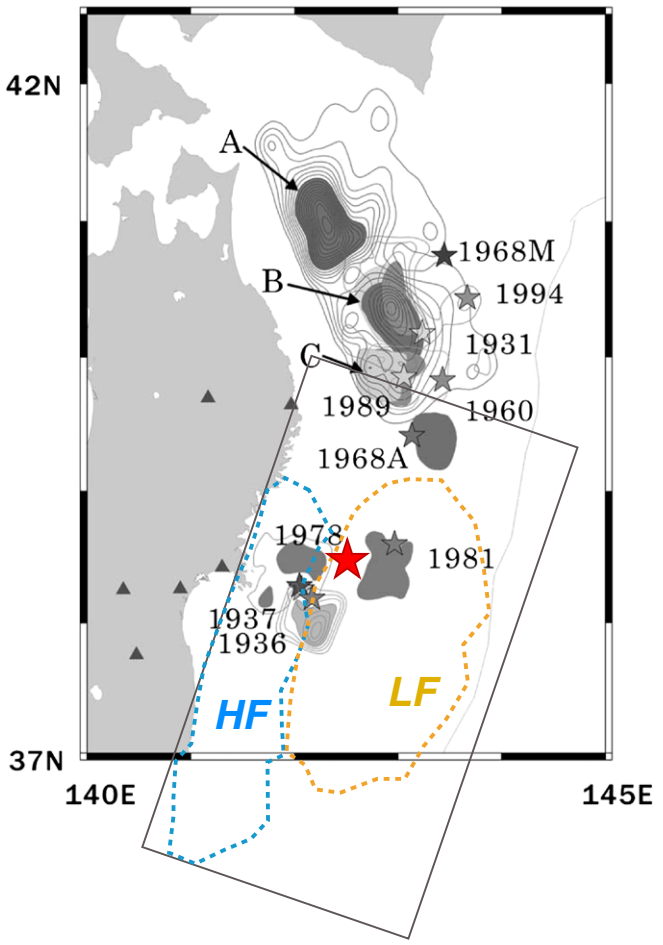

Fig. 2. Asperity distribution (shown by dark shading) estimated from the analysis of 10 large earthquakes which occurred in the 20th century. Stars show the main shock epicenters. The contour lines show the moment release distribution. The rectangle indicates the rupture region for the 2011 Tohoku-Oki earthquake, and the dotted contours the areas of dominant high-frequency radiation down-dip and dominant low-frequency radiation up-dip, respectively.
Modified after Yamanaka and Kikuchi (2004).

gsi.go.jp/UJNR/6th/orally/O01_UJNR_Dobashi.pdf). Some other studies suggested that only a fraction of the accumulated tectonic stress was being relieved during the historical earthquakes, and that there was a possibility of larger events with source areas that combine the faulting regions of the known past earthquakes (Igarashi et al., 2003; Kanamori et al., 2006). There are also studies of tsunami deposits associated with the A.D. 869 Jogan and other earthquakes that indicated the occurrence of past large tsunamis near Sendai bay and broader areas in the south (Minoura et al., 2001; Shishikura et al., 2007, 2010).

Following the 1995 Kobe earthquake (Mw 6.8; 6437 fatalities, and very large economic losses), Japan installed many observation networks, including borehole seismic arrays, dense strong-motion instrumentation, extensive GPS arrays, and real-time earthquake information systems (Okada et al., 2004). The advance in seismological studies and preparations for earthquake hazards have been significant. The excellent distribution of seismic stations and many earthquake sources have enabled high resolution seismic tomographic results and detailed source models of recent earthquakes. Nonetheless, the potential of a Mw 9 earthquake was not broadly recognized.

The main damage from the 2011 Tohoku-Oki earthquake was caused by the very large tsunamis that inundated several hundred kilometers of coastlines of northeast Honshu with heights of 10 to 30 m. Tsunamis completely destroyed many coastal towns in Miyagi and Iwate prefectures, and caused the much publicized failure of a nuclear power plant in Fukushima. The Japan Meteorological Agency (JMA) issued warnings for tsunamis 3 min after the origin time (Ozaki, 2011), which should have provided sufficient time for most people to escape. However, complications in the communication and emergency response caused problems so that many people were killed by the huge onrush of water. Tsunamis caused an estimated damage of over $US 300 billion and took about 19,000 lives.

The amount of shaking damage was not great, especially compared to other similar size earthquakes, despite the very high levels of ground motion from the sources fairly close to the coast (peak accelerations of over 2 g at many sites). Just 4.4% of the reported deaths are from building collapses and landslides. The low levels of shaking damage can be attributed to relatively low amplitudes in the critical frequency range of 0.5 to 1 Hz (e.g. Furumura et al., 2011) combined with the high standards of building construction in Japan.

The initial epicenter of the Mw 9 event was about 100 km off the coast of Miyagi prefecture; the first P arrivals were detected about 22 s after the occurrence. The earthquake early warning (EEW) system of JMA issued an alert for strong ground shaking due to the earthquake 8 s later (Hoshiba et al., 2011). Systems in factories were shut down automatically, bullet trains were slowed and stopped, and warnings were sent out on TV and cellular phones.

Two days before the March 11 earthquake, a Mw 7.3 event occurred in the same subduction zone, off the coast of the Miyagi-prefecture. This March 9 event turned out to be a foreshock to the much larger Mw 9 earthquake on March 11. The foreshock sequence was the beginning of a process where many sections of the subduction zone along the Japan Trench ruptured in a single sequence, which was unprecedented in the historical record of the past 400 years. When the rupture sequence started, the tectonic stress levels in previously distinct source areas may have been close to the maximum shear strength for these zones. This condition promoted complex rupture propagation through the broad region producing the huge Mw 9 event (e.g., Tajima and Kennett, 2012).

Numerous papers have already been published studying the characteristics of the 2011 Tohoku-Oki megathrust earthquake using the abundant data and advanced methods of analyses. This review focuses on several important issues from a viewpoint of earthquake hazard mitigation practice. We summarize the characteristics of this megathrust event and the associated physical properties of the structure in comparison with the past characterizations of seismic activities in this subduction zone, and the progress of real-time forecasting system of strong ground shakings and tsunamis. We also address how the potential of an impending large earthquake and associated tsunamis might be detected.

2. Characterizations of large earthquakes prior to the 2011 Tohoku-Oki earthquake

Past seismic activity known from historical documents and instrumental records had led to the assumption of characteristic large earthquakes for the region of the 2011 Mw 9 earthquake and the surrounding region.

2.1. Historical large earthquakes

Systematic instrumental observations and recordings of seismic events started around the turn of the 20th century. Investigation of seismic activity prior to the instrumental era depends entirely on historical documents and paleoseismological investigations, where available information is limited and inhomogeneous in terms of spatial and temporal coverage. The subsequent estimates of earthquake or tsunami size, as well as the recurrence intervals of such events can be quite uncertain. Nonetheless, the historical catalogs of large earthquakes in Japan,

which span over 1500 years including the A.D. 648 Hakuho earthquake (estimated as M ~8.4) along the Nankai trough, are fairly well compiled for the purpose of identifying possible large earthquake and tsunami risks (see the web site of the Seismological Society of Japan, SSJ: http://www.zisin.jp/modules/pico/index.php?cat_id=100).

The historical catalog shows that there was a significant earthquake with an associated large tsunami that occurred along the northeast coast of Honshu during the Jogan era (in A.D. 869), and was estimated to be M 8.3 or larger. The tsunami deposits associated with this earthquake were found 1 to 3 km from the coast in the Sendai area (Minoura et al., 2001; Shishikura et al., 2007, 2010). A simulation study of the tsunami inundation attempted to determine the source area of this earthquake using several different types of tsunami source models (Satake et al., 2008). Based on these studies, the Jogan earthquake in 869 is considered to be similar to the 2011 Tohoku-Oki earthquake. During the 17th to 19th century there are 8 M ≥7 earthquakes, and 4 M ≥8 earthquakes known in this region (Fig. 1). The Keichou Sanriku earthquake (M ~8.1) occurred in 1611 and is considered to have had a similar mechanism to that of the 1933 Showa Sanriku earthquake (M ~8.1) based on the nature of tsunami damage. Here, we note that the 1933 earthquake is a normal fault event in the outer-rise. However, there are controversies regarding the epicenter of the 1611 earthquake, which could be located off the coast of Hokkaido, farther north of Sanriku-Oki. The 1896 Meiji Sanriku-Oki earthquake (M ~8.2) is considered as a thrust event in the subduction zone. The occurrence rate of large earthquakes (M ≥7) during this period is less than that observed during the past century (see below), indicating that the historical catalog is not homogeneous or the seismic activity is not regular over a period of 400 years.

2.2. Large earthquakes over the last century

Over the last century there are 14 M 7 earthquakes and 2 M 8 earthquakes (the M 8.1 normal faulting event in 1933 and the Mw 8.2 1968 Tokachi-Oki subduction zone event) that took place off the coast of the Tohoku region. Yamanaka and Kikuchi (2004) collected strong-motion waveform data for 10 large interplate earthquakes archived by JMA and determined the source processes of these earthquakes. These events typically show a complex source rupture process (see also Seno et al., 1980), but the conditions may not have been mature enough for the rupture propagation to break through a broad region, as was the case in the 2011 earthquake. The ruptured segments of these past events range from 50 to 150 km. Yamanaka and Kikuchi (2004) identified large slip areas (asperities) for the earthquakes which occurred after 1930. They suggested that the typical size of individual asperities, which are distributed sparsely in this region, was associated with an M 7 earthquake, and M 8 earthquakes occurred when several asperities ruptured together (see the asperity map in Fig. 2).

The estimated rupture areas for the past large earthquakes in this region up to 2011 show two distinct groupings. There is a group of events near the trench axis that have been associated with major tsunamis; these events lie to the northeast of the epicenter of the 2011 March 11 event. There is also a more southerly group at greater depth and closer to the coastline (Koper et al., 2011a; see Fig. 3).

Using historical records for over 400 years, a wide range of probabilities for large subduction earthquakes was estimated for M 7 to M 8 earthquakes in this subduction zone (ERC). However, Kanamori et al. (2006) also recognized that only part of the accumulated strain associated with subduction had been relieved despite the significant earthquake activity along the east coast of Honshu. They pointed out the potential of an event that would combine the areas and characteristics of the two groups of prior events noted above. This is the character of the 2011 Tohoku-Oki event, with large lower-frequency radiation near the trench and higher-frequency radiation down-dip from the epicenter (see Section 3).

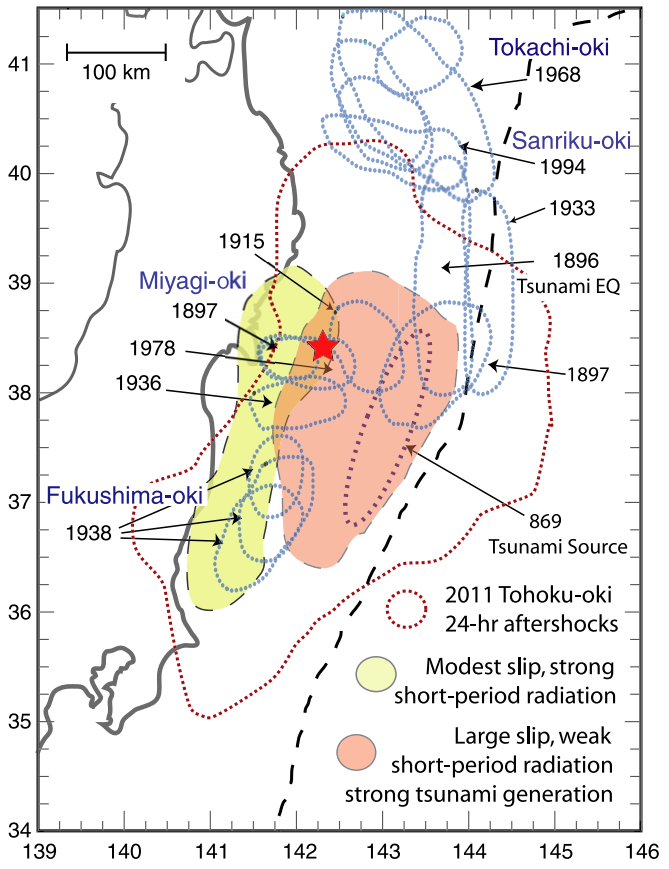

Fig. 3. Locations of the source areas of historic offshore large earthquakes along the Tohoku coast (blue ellipsoidal shapes by Kanamori et al., 2006) on a schematic map of inferred fault zone rupture segmentation for the 2011 Mw 9 Tohoku-Oki earthquake. The yellow colored region is where co-seismic short-period radiation with relatively low seismic moment is imaged. The orange-colored region is where there is little short-period radiation, but large slip is placed in broadband finite fault inversions of seismic and geodetic data. The approximate location of the A.D. 869 Jogan tsunami source region (Minoura et al., 2001) is found to lie within the region of large slip. Here the 2011 main event epicenter by USGS is indicated with a red star, and the 1-day aftershock area by red dots, including outer rise activity beyond the region of large slip (from Koper et al., 2011a).
Reproduced/modified by permission of Earth, Planets and Space.

2.3. Aftershock activity of past large earthquakes and repeating small events

After the main source rupture is complete, there is an expansion of aftershock activity reflecting stress adjustment and migration, if the areas of large slip are surrounded by weaker zones. Tajima and Kanamori (1985a, 1985b) characterized the plate coupling strength (or asperity) distribution along the major subduction zones world-wide using the spatial expansion patterns of aftershocks with time, using the amount of seismic energy released from aftershocks per unit area and unit time. To quantify the global results, a linear expansion ratio η_l for the characteristic size of the aftershock zone, and an areal expansion ratio η_s, are calculated as a function of time. The ratios are calculated from the size at a certain time after the mainshock t_{aft}(day) divided by the 1-day aftershock area, where the 1-day aftershock area is considered to represent the rupture area of the earthquake. The results indicate that typical expansion patterns of aftershock areas can be classified into three groups: (1) very little expansion associated with a megathrust earthquake, e.g., the 1964 Alaskan earthquake (Mw 9.2); (2) little expansion along the strike and some expansion in the dip direction, e.g., large events in the Kurile subduction zone; and (3) large areal and linear expansions, e.g., the 1978 Miyagi-Oki (Mw 7.5) earthquake in northeast Japan and the

1968 Molucca Sea earthquake (Ms 7.6) in the southwestern Pacific subduction zones.

In group 3 relatively small asperities are distributed sparsely and the aftershock activity expands significantly into the surrounding weaker zones, with aftershock areas often overlapping with those of past adjacent events. Large events (Mw ~7 to 8) off the coast of northeast Japan during the past century have shown such significant expansion of aftershock activity into the surrounding areas over time ($\geq t_{aft}(100)$). This pattern is in contrast to a subduction zone that is characterized by uniform, large asperities (group 1), which produce megathrust events, such as the 1964 Alaska earthquake (Mw 9.2) that ruptured a large portion of the plate boundary with a characteristic source-time of $\tau \sim 180$ s. The aftershock area of the 1964 Alaska earthquake did not show much expansion over time ($t_{aft} \geq 100$ days) and the inter-plate coupling was considered strong.

The weaker zones surrounding the asperities were also considered likely to be broken by repeating small events (e.g., Igarashi et al., 2003; Matsuzawa et al., 2002, 2004; Uchida et al., 2004). However, Igarashi et al. (2003) compared repeating earthquake data with the

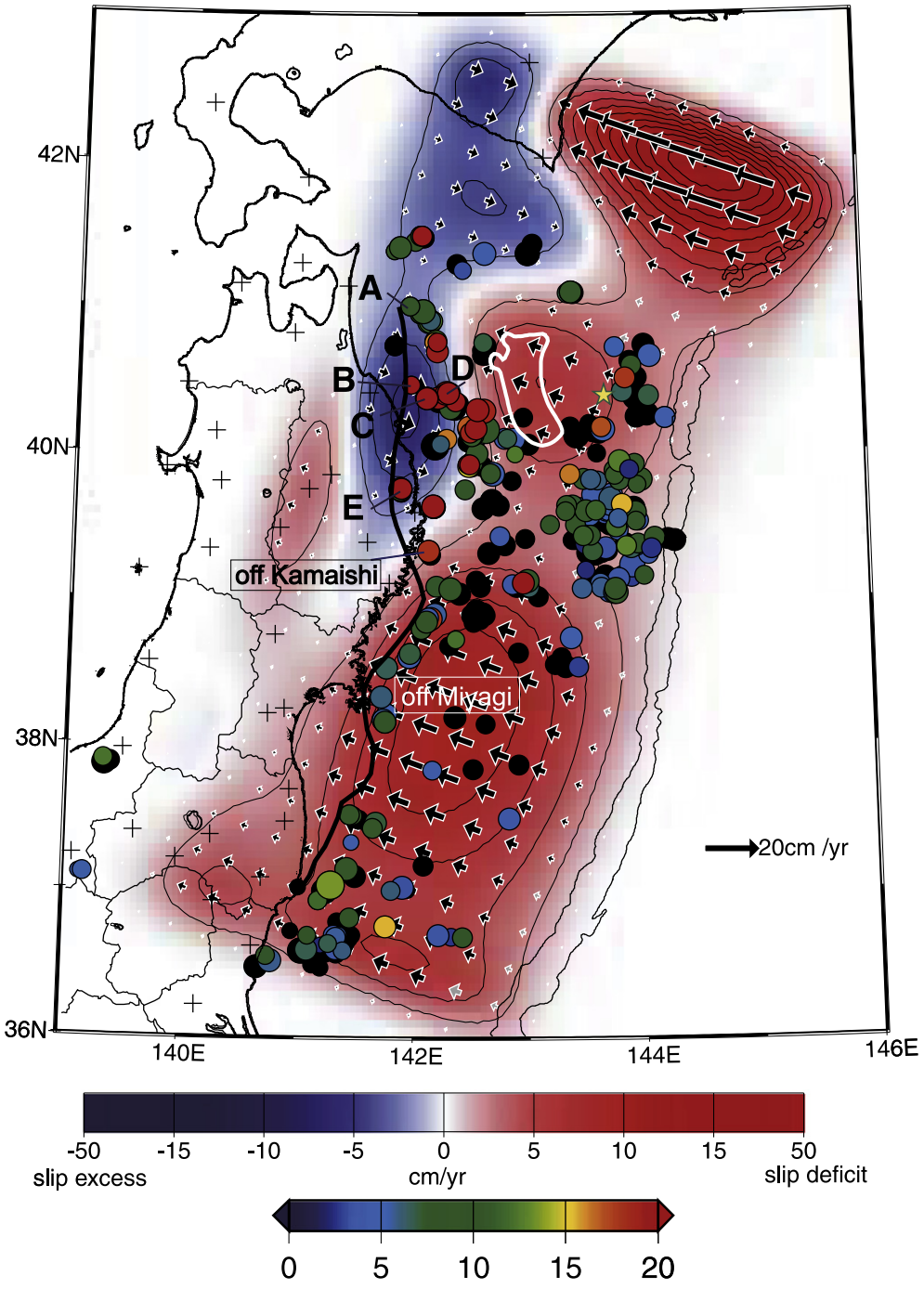

Fig. 4. Repeating earthquake data compared with the slip rate distribution on the plate boundary estimated from GPS data for the period from April 1996 to March 1999 analyzed by Nishimura (2000). Solid colored circles show the locations of repeating earthquake clusters, and their colors show average slip rate. The slip rate distribution obtained from the GPS analysis is shown by contours with an interval of 2 cm/yr. Red shows a slip deficit (e.g., strongly coupled) area, and blue is a slip excess (e.g., slip rate is larger than the interplate convergence rate) area. Arrows indicate the amount of slip (from Igarashi et al., 2003; see this paper for details).
Reproduced/modified by permission of American Geophysical Union.

slip rate distribution on the plate boundary estimated from GPS data by Nishimura (2000) and discussed the slip deficiency in relation to repeating small earthquakes (Fig. 4; see also Nishimura et al. (2000)).

3. Characteristics of the mainshock and aftershock activity

Seismic, geodetic and tsunami data for the 2011 Tohoku-Oki event were readily available from around the world. Strong ground motion was recorded by over 1000 near-field stations in Japan, and teleseismic data were obtained worldwide, including data from multiple large-aperture arrays. Within a few days, a number of preliminary source models were presented on webpages around the world using various sources of data. The first source models were obtained from primarily teleseismic seismic data because of the easy availability of the data.

3.1. Real-time information

In Japan an Earthquake Early Warning (EEW) system has been operated by JMA since October, 2007. The hypocenters are determined by a combination of several techniques (Hoshiba et al., 2008), using approximately 1100 stations from the JMA network and the Hi-net network of NIED. The system locates 10–20 events per day within a few seconds, which includes a few felt earthquakes in and around Japan, and issues warnings when strong ground shaking is expected. One procedure to obtain a fast location uses a technique that identifies both stations that record P arrivals and stations where the P waves have not yet arrived (Horiuchi et al., 2005). The system is able to locate earthquakes within a few seconds and detect erroneous arrival-time readings. As more information becomes available with time, locations and magnitude are updated every second.

At 14:46:40.2 on 2011 March 11 the EEW system detected P-wave first motion arrivals and issued an alert for strong ground shaking due to a large earthquake estimated to be M ~7.9, and the warning was automatically broadcast through TV, radio and cellular phone alarms. The alert was issued to a broad region where intensity 5 or greater on the JMA scale was estimated to occur. The warning was sent to this region more than 15 s before the arrivals of the S-wave and the strong ground motion (Hoshiba et al., 2011). However, in many affected areas the actual intensities were substantially larger than the estimated intensities. The underestimate of magnitude and intensity can be attributed to the long duration and growth of the rupture process over a very large rupture area, and limitations in the algorithm

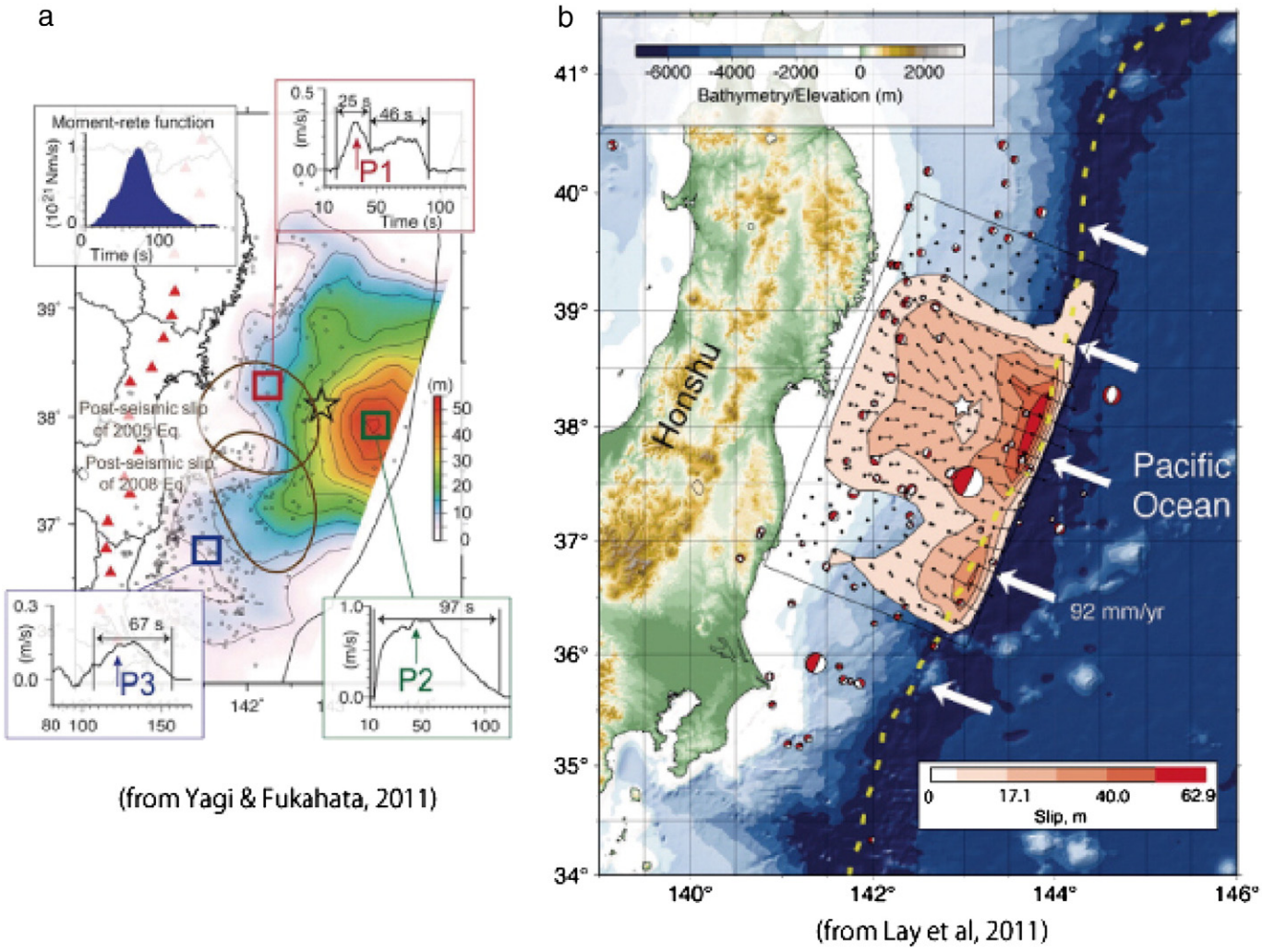

Fig. 5. Slip distributions determined for the 2011 Tohoku-Oki main event (with its epicenter denoted by a star) from teleseismic P-wave data: (a) Map view of the total slip distribution, moment-rate function, and slip-rate functions at three locations (indicated with red, green and navy small squares) obtained using a newly developed inversion method of Yagi and Fukahata (2011a). The maximum slip of about 50 m is determined near the trench (see Yagi and Fukahata, 2011b for details of the method). (b) Slip model P-MOD2 obtained from least-squares inversion of teleseismic P-waves. The yellow dashed curve indicates the position of the trench deep and the white arrows the relative plate motion of the Pacific plate, holding the Japan mainland fixed (Lay et al., 2011a).
Reproduced/modified by permission of American Geophysical Union; and Earth, Planets and Space.

for determination of earthquake parameters, which assumes a point source. The underestimated magnitude was revised to M 8.4 in 80 min, and to M 9.0 several days later.

The U.S. Geological Survey National Earthquake Information Center (USGS NEIC) worked rapidly to determine a Mw of 8.9 within 20 min and in a few hours had characterized the earthquake in terms of its location, size, faulting source, shaking and slip distribution (Hayes et al., 2011). The mainshock source had a seismic moment of 4.5×10^{22} Nm (Mw 9.0); the source duration (τ) of 150 s; and thrust focal mechanism (strike = 200°, dip = 13°, rake = 83°).

3.2. Slip distribution models

Following the earthquake, there were many websites reporting slip distribution models, using mainly teleseismic waveforms and regional GPS data. Data for these studies were readily available from networks such as the Federation of Digital Seismograph Networks (FDSN) and Global Seismographic Network (GSN) and distributed at data centers including the Data Management Center (DMC) of Incorporated Research Institutions for Seismology (IRIS).

Hayes (2011) reports that fast finite-fault inversions with globally distributed body- and surface-wave data were used to estimate the slip distribution of the earthquake rupture. Models generated within 7 h of the earthquake origin time indicate the rupture of a fault up to 300 km long, which was roughly centered on the earthquake hypocenter, and involved peak slips of 20 m or more. Updates since this preliminary solution improved the details of this inversion solution, and thus the understanding of the rupture process.

Published models for the mainshock source can show notable differences depending on the specific sources of information employed. Common to most of the results using seismic and GPS data, is the very large slip near the hypocenter and eastward toward the trench. Fig. 5 compares the slip distributions determined by two studies using teleseismic P-waves, (a) Yagi and Fukahata (2011a) and (b) Lay et al. (2011a). Both of the models show a large slip area in the up-dip direction from the hypocenter with maximum slip of over 40 m near the trench. Studies of regional strong motion data on the Japanese islands (e.g., Furumura et al., 2011; see Fig. 6) revealed a series of major subevents of different spectral characteristics (see also Nakahara et al., 2011).

An interesting feature that is noted in many models is the difference between the area associated with large low-frequency radiation located near and up-dip from the hypocenter, and the area of dominant high-frequency radiation located down-dip of the hypocenter (Ide et al., 2011; Kiser and Ishii, 2012; Koper et al., 2011a, b; Wang and Mori, 2011a,b). The largest slip, and thus the source of the low-frequency (<0.1 Hz) energy lies in the region of the hypocenter and trenchward on the shallow portion of the fault, while the sources of the high-frequency energy (1 to 10 Hz) were on the deeper down-dip portions of the fault (e.g. Kurahashi and Irikura, 2011; Wang and Mori, 2011a). The source regions for the intermediate frequencies appear to have a more complicated spatial distribution. The locations of the high-frequency sources are important for evaluating strong-motions that cause damage to small to moderate size structures.

Table 1 summarizes the source models in published papers as of February 2012. Many studies determined the seismic moment for the earthquake with most values in the range of 4.0 to 6.0×10^{22} Nm, which corresponds to Mw 9.0 to 9.1. Most models show a large patch with dimensions of about 200 km and slip of 30 to 60 m. This large slip on the shallow up-dip portion of the thrust fault (in deep water) is responsible for a large part of the tsunami generation. The seismic moment for the Tohoku earthquake is similar or slightly less than the 2004 Sumatra earthquake, but the fault is about half the area. This implies that the average amount of slip was about twice that of Sumatra.

Source models using only tsunami data tend to give larger values of slip for the shallow portion of the fault near the trench (Fujii et al., 2011; Maeda et al., 2011; Saito et al., 2011). This raises the possibility of a slow or late component of the slip that may not be seen in the seismic data. Also, the distribution of very large tsunami heights onshore of Iwate prefecture seems to indicate large sea floor

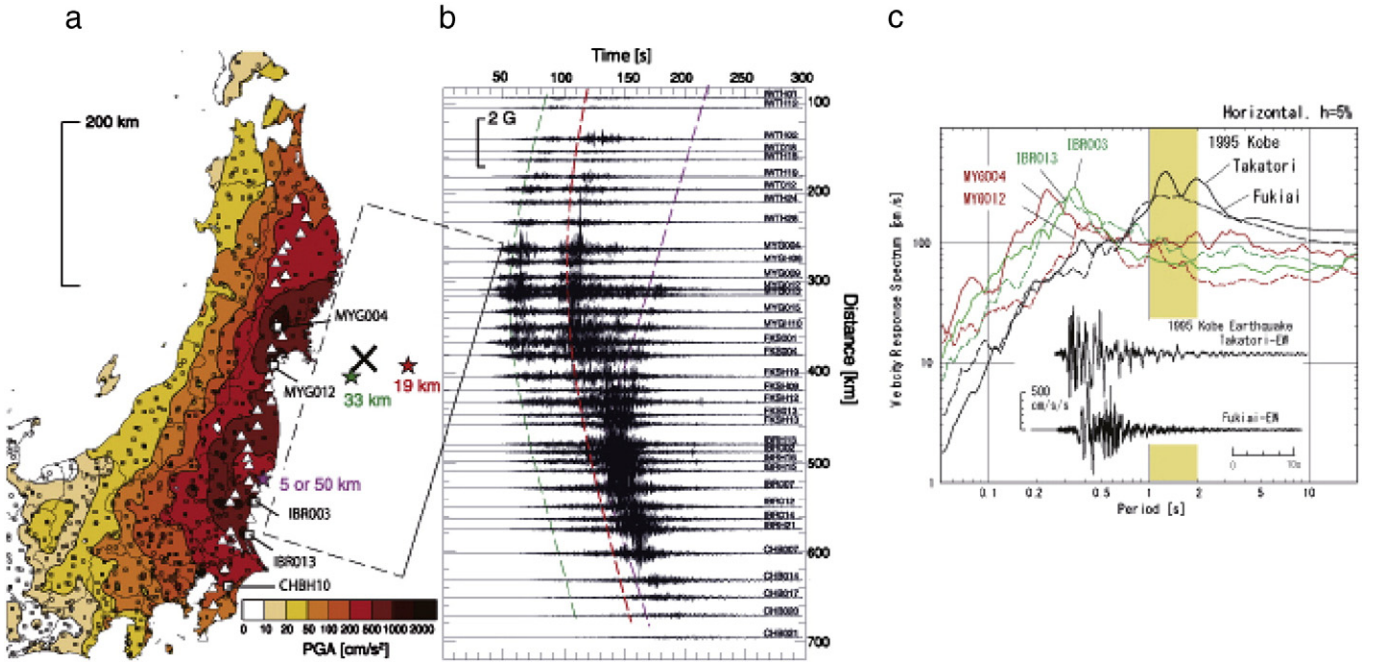

Fig. 6. Direct observation of strong ground motions: (a) Distribution of peak ground acceleration (PGA; cm/s/s). Three locations of large slips are indicated with green, red, and purple stars. (b) Record section of the vertical component ground acceleration recorded at linearly aligned 42 stations from north to south (white triangles shown in (a)). The dashed curves (green, red, and purple) correspond to the theoretical arrival times of three subsources in (a). (c) Velocity-response spectra of horizontal ground motions recorded at four stations shown with squares in (a). The spectra are compared with those obtained at Takatori and Fukai during the 1995 Mw 6.8 Kobe earthquake. The yellow-highlighted period band (1–2 s) corresponds to the most effective period for wooden-frame houses (assembled after Furumura et al., 2011).
Reproduced/modified by permission of Landslides.

Table 1
Summary of source models for the 2011 Tohoku earthquake.

Reference	Data	Moment (10^{22} Nm)	Mw	Max. slip (m)	Comment
Duputel et al., 2011	Tele body and surface waves		9.0		Rapid moment determination, W phase
Hara, 2011	Tele body waves				Duration of high-frequency
Hayes, 2011	Tele. body and surface waves	4.9	9.1	>32	Rapid moment determination
Ide et al., 2011	Tele. body waves			30	Frequency dependence
Ishii, 2011	Tele body waves				Back projection
Koper et al., 2011a	Tele body waves				Back projection, frequency dependence
Lay et al., 2011b	Tele body waves	4.0	9.0	60	Source inversion
Meng et al., 2011	Tele body waves				Back projection, frequency dependence
Nettles et al., 2011	Tele surface waves	5.3	9.1		Low-frequency moment
Polet and Thio, 2011	Tele surface waves		8.9–9.0		Rapid moment determination
Roten et al., 2012	Tele surface waves				Back projection
Shao et al., 2011	Tele body and surface waves	5.8	9.1	60	Source inversion
Tsai et al., 2011	Tele surface waves	4.2	9.0		Low-frequency moment
Wang and Mori, 2011a	Tele body waves				Back projection
Wang and Mori, 2011b	Tele body waves				Back projection, frequency dependence
Yagi and Fukahata, 2011a	Tele body waves	5.7	9.1	50	Source inversion
Yao et al., 2011	Tele body waves				Back projection, frequency dependence
Zhang et al., 2011	Tele body waves				Back projection
Honda et al., 2011	Regional strong-motion data				Back projection
Hoshiba and Iwakiri, 2011	Regional strong-motion data				Early warning
Hoshiba et al., 2011	Regional strong-motion data				Early warning
Kurahashi and Irikura, 2011	Regional strong-motion data				Location of high-freq. sources
Nakahara et al., 2011	Regional strong-motion data				Back projection
Suzuki et al., 2011	Regional strong-motion data	4.4	9.0	48	Source inversion
Yoshida et al., 2011a	Regional strong motion, Tele body waves	3.4	9.0	>25	Source inversion
Yoshida et al., 2011b	Regional strong-motion data	4.3	9.0	47	Source inversion
Iinuma et al., 2011	GPS	4.0	9.0	35	Source inversion
Ito et al., 2011b	GPS	4.1	9.0	60	Source inversion
Miyazaki et al., 2011	GPS			35	Source inversion, foreshock and mainshock slip
Nishimura et al., 2011	GPS		8.9	41	Forward modeling
Ozawa et al., 2011	GPS	4.1	9.0	60	Source inversion
Pollitz et al., 2011	GPS	4.1	9.0	33	Source inversion
Simons et al., 2011	GPS, Tele body waves			45 to 60	Source inversion, Back projection, Frequency dependence
Yue and Lay, 2011	High-rate GPS	4.8	9.1	60	Source inversion
Kido et al., 2011	Ocean bottom pressure			80	Forward modeling
Fujii et al., 2011	Tsunami	3.8	9.0	>40	Source inversion
Maeda et al., 2011	Tsunami			57	Forward modeling
Saito et al., 2011	Tsunami		9.0	30	Source inversion
Yamazaki et al., 2011	Tsunami, GPS			60	Source inversion
Ammon et al., 2011	Tele. body and surface waves, high-rate GPS	3.9	9.0	40	Source inversion
Koketsu et al., 2011	Tele body waves, Regional strong motion, GPS, Tsunami	3.4 to 3.8	9.0	36 to >40 m	Source inversion
Koper et al., 2011b	Tele body and surface waves, high-rate GPS			42	Source inversion, back projection, frequency dependence
Lee et al., 2011	Tele body waves, regional strong motion, GPS	3.7	9.0	>50	Source inversion
Yokota et al., 2011	Tele body waves, regional strong motion, GPS, tsunami	4.2	9.0	35	Source inversion

deformation north of the area of large slip identified in the models using seismic and GPS data.

Combining multiple types of data helps constrain the overall features of the source models and reduces resolution problems inherent to a particular data set. For example, onshore GPS data is less sensitive to fault displacements far offshore, and regional seismic data is better for constraining rupture propagation than teleseismic data. Inversion studies that used different types of data sets to obtain source slip distribution models include, Ammon et al. (2011), Koketsu et al. (2011), Koper et al. (2011b), Lee et al. (2011), Yokota et al. (2011) and others.

Studies of the rupture propagations using finite fault inversions (Ide et al., 2011; Koper et al., 2011a,b; Meng et al., 2011) and back-projection methods (Ishii, 2011; Kiser and Ishii, 2012; Koper et al., 2011a, b; Wang and Mori, 2011a, b; Yao et al., 2011; Zhang et al., 2011) with teleseismic data, and regional data (Furumura et al., 2011; Kurahashi and Irikura, 2011; Nakahara et al., 2011) show complex patterns for the time evolution of the earthquake, especially during the first minute. Different studies give different results about the direction and rupture speed for the early portion of the earthquake and there are some indications that the rupture may have reversed itself and re-ruptured a portion of the fault. After about the first minute, most results show unilateral rupture propagation toward the southwest.

3.3. Crustal stress accumulation and release

Looking at the results from the many slip distribution models, an important issue is the location on the fault and the areal extent of the large slip. How far towards the trench did the large slip occur? Did the slip occur mainly on the near-horizontal megathrust or on steeply dipping faults? Most of the source models show large slip on the shallow portion of the fault close to the trench, but seismic and GPS models do not have good resolution for these far-offshore regions.

The 2011 Tohoku-Oki earthquake produced the largest ground deformations directly measured for an earthquake, which were observed on the ocean floor near the epicenter and trenchward toward the east, with horizontal movements of 24 to 74 m (Ito et al., 2011a, in press;

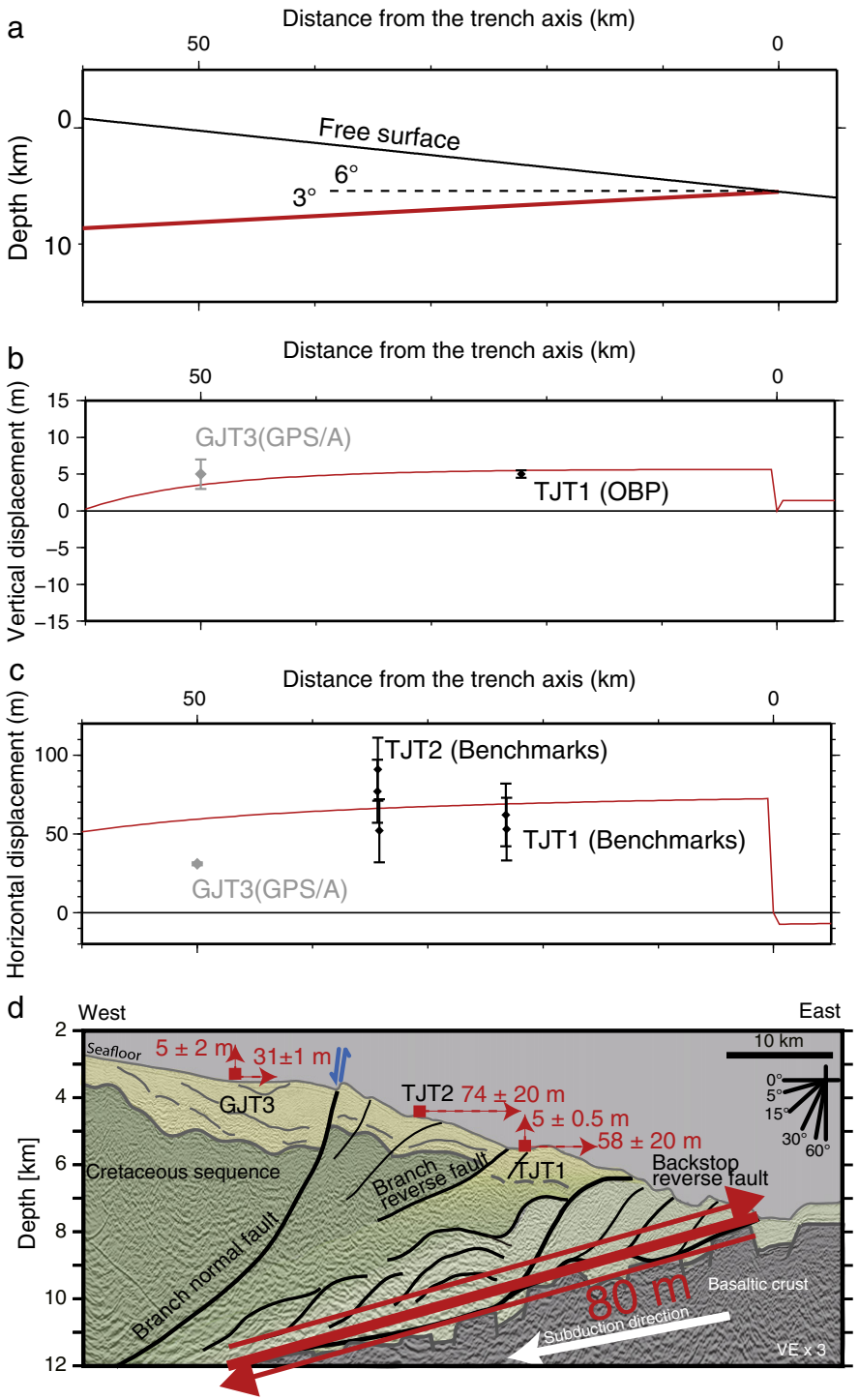

Fig. 7. Direct observation of deformation for the frontal wedge near the 2011 Tohoku-Oki earthquake source measured by cabled seafloor pressure gauges and corresponding modeling. (a) Two-dimensional fault model along a profile perpendicular to the trench axis. Comparison between observed (diamonds) and predicted (red curves) displacements for (b) vertical, and (c) horizontal components, respectively. (d) Pre-existing seismic structure and observed deformation of the frontal wedge. The seismic structure is modified from Tsuji et al. (2011). Observation sites TJT1, TJT2, and GJT3 are indicated (see Ito et al., 2011a, in press for the detail).
Reproduced/modified by permission of American Geophysical Union.

Kido et al., 2011; Sato et al., 2011). Fig. 7 shows the deformation near the frontal wedge of the Tohoku-Oki earthquake measured by cabled seafloor pressure gauges, and the modeling that indicates an uplift of 5 m with a horizontal displacement of more than 60 m (Ito et al., 2011a, in press). The results suggest a huge coseismic slip beneath the frontal wedge on the plate boundary, which could be as large as 80 m. Another piece of convincing evidence is from differential bathymetry on a profile before and after the earthquake (Fujiwara et al., 2011), which shows there was a large and mainly horizontal displacement out to the tip of the thrust, indicating that slip occurred mostly on the megathrust itself, rather than splay faults. In the case of the 2004 Sumatra–Andaman earthquake the coseismic uplift was followed by postseismic subsidence within two months after the earthquake (Kayanne et al., 2007).

Models of the deformation in the region of the accretionary prism, at the tip of the thrust, usually assumed that this area does not accumulate

stress because of the weak strength of the materials (e.g. Wang and Hu, 2006). Slip on this portion of the plate boundary megathrust is often thought to occur aseismically, so that large displacement in this region is not expected during great subduction zone earthquakes. The 2011 Tohoku-Oki earthquake has shown that this toe region can have a large amount of slip during an earthquake. This raises questions about mechanisms for earthquake reoccurrence and large slip on this shallow portion of the fault. Was the stress at a high level, having accumulated for over a thousand years and then released in the recent earthquake, or was the accumulated stress at a low level and the large slip due to overshoot or some other mechanisms that couples the shallow portion of the fault with the deeper part of the fault? A recent study of the shallow portion of the megathrust for the 2004 Sumatra earthquake also suggests large displacement for this toe region (Singh et al., 2011).

The amount of accumulated stress on the megathrust before the 2011 Tohoku-Oki earthquake has been discussed from studies of GPS observations by Nishimura et al. (2004), Suwa et al. (2006), Hashimoto et al. (2009), and Loveless and Meade (2010). These studies identified areas of slip-deficit rates that might be expected to rupture in large earthquakes. For example, areas of strong coupling may be associated with earthquakes in 1931 Sanriku-Oki (M 7.6), 1968 Tokachi-Oki, 1994 Sanriku-Haruka-Oki (Mw 7.8) for the region north of the 2011 Tohoku-Oki earthquake (Hashimoto et al., 2009). Hashimoto et al. (2012) inverted interseismic GPS velocity data and the coseismic GPS displacement data to show that the 2011 main event released tectonic stress accumulated in the Miyagi-Oki and Fukushima-Oki interseismic slip-deficit zones extending from 36°N to 40°N off the Pacific coast of the Tohoku district. The extraordinarily large coseismic slip in the Miyagi-Oki slip-deficit zone, where previous large earthquakes with about 3 m coseismic slip repeated every 40 yr over the last two centuries, indicates that the region can have different size asperities with varying amounts of slip for different earthquakes (Hashimoto et al., 2012). These GPS studies have shown large slip deficit off Miyagi-Oki and Fukushima-Oki prior to the 2011 main event, but could not detect large slip deficit accumulated near the trench.

Ozawa et al. (2011) reported the coseismic and postseismic slip using recent geodetic data from the GPS network (see Fig. 8), and pointed out that the strain accumulation rate estimated in the Tohoku-Oki source region is much higher than the average rate of strain release from previous interplate earthquakes. They suggest that the 2011 Tohoku-Oki earthquake released the strain accumulated for several hundred years, which may have resolved part of the strain budget imbalance.

3.4. Similarity to tsunami earthquakes

'Tsunami earthquakes' are a special class of shallow subduction-zone events that have relatively low levels of energy in the frequency range that is easily perceptible to people (1 to 10 Hz), but large (shallow) fault displacement, thus producing large tsunamis, (Fukao, 1979; Kanamori, 1972). Although the 2011 Tohoku-Oki earthquake is not considered to be a tsunami earthquake by most seismologists, the event does have some of features associated with tsunami earthquakes, such as a low rupture velocity for a portion of the source process (e.g., Meng et al., 2011; Yagi and Fukahata, 2011a). Also, the radiation efficiency (ratio of radiated energy to radiated plus fracture energy) is rather low, especially for the region of large slip, similar to tsunami earthquakes. This indicates that the amount of energy in the seismic waves for the 2011 Tohoku-Oki event is rather small when compared to other great earthquakes (Lay and Kanamori, 2011). The earthquake has characteristics of a 'tsunami' earthquake for the large slip on the shallow portion of the fault, and resembles a typical plate boundary subduction-zone earthquake for the deeper portions of the rupture area. Lay and Kanamori (2011) point out that the shear sliding on the fault shifted the coast of Japan up to 5 m eastward, and lifted the sea floor by as much as 5 m over 15,000 km^2; displacements as large as 30 to 60 m – the largest ever measured for an earthquake – occurred near the subduction trench.

Recently there has been much focus in Japan on the possibility of future M 9 earthquakes, especially related to the possibility for future

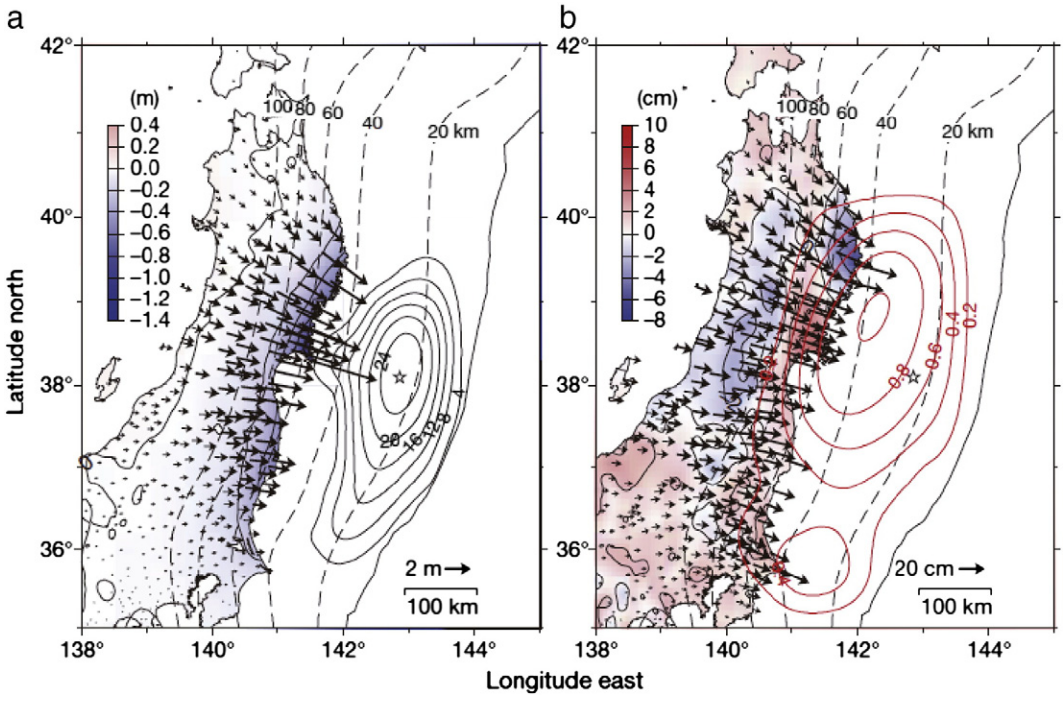

Fig. 8. Coseismic and postseismic displacement observations and estimated slip, relative to the Fukue site (off the west coast of Kyushu): (a) Coseismic displacements for 10–11 March 2011. The arrows indicate the horizontal coseismic movements of the GPS sites. The color shading indicates vertical displacement, and the star the main event epicenter. The solid contours show the estimated coseismic slip distribution in meters. (b) Post seismic displacements for 2011 March 12–25. The red contours show the afterslip distribution in meters (from Ozawa et al. (2011)).
Reproduced/modified by permission of Nature.

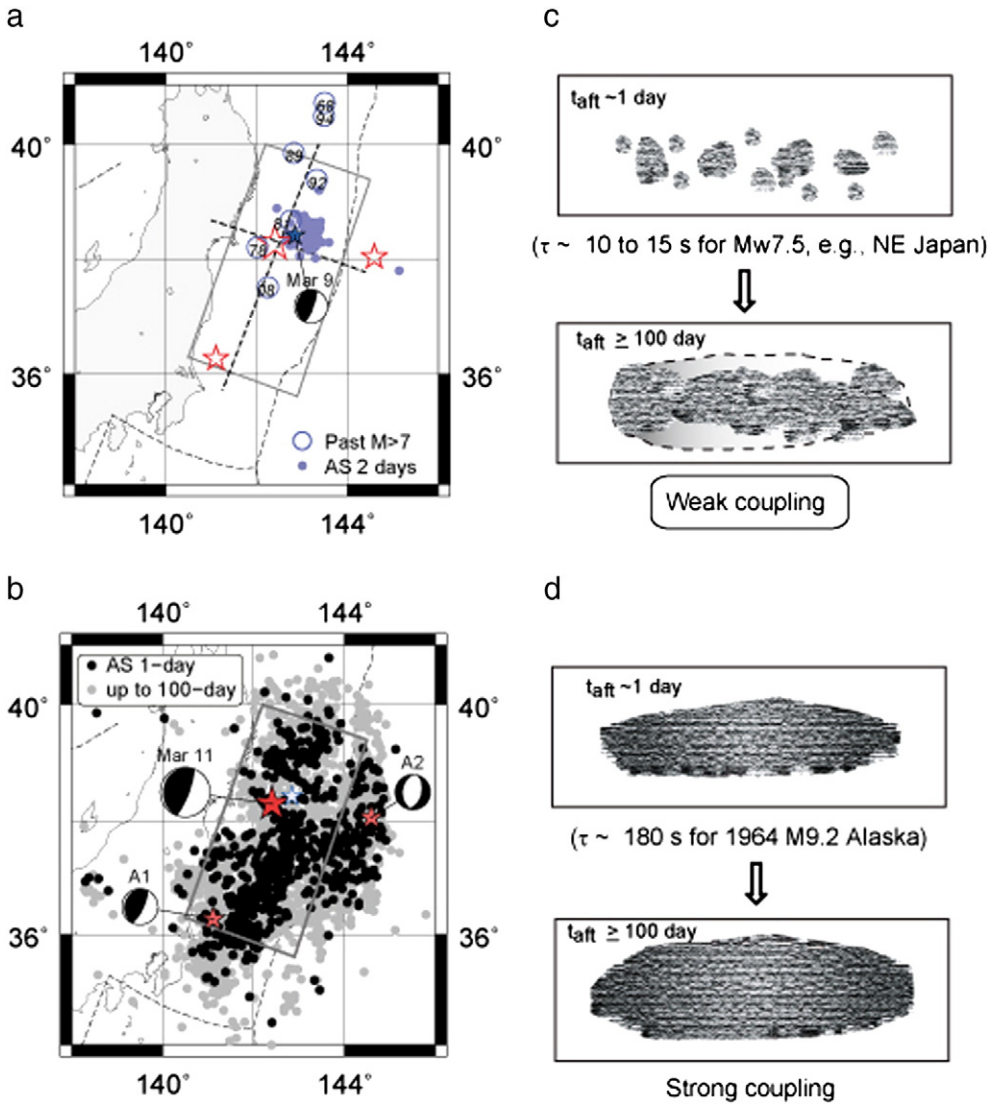

Fig. 9. Aftershock activity of the 2011 Tohoku-Oki earthquake and illustration of typical aftershock area expansion patterns associated with the asperity distribution: (a) The immediate aftershocks of the Mw 7.3 event on March 9 are located mainly to the east of the epicenter (light blue star). Large earthquakes (M ≥ 7) in the past half century are also shown (open circles in light violet). The ruptured area of the March 11 event is outlined by a gray rectangle. The red open stars indicate the epicenters of the Mw 9 event and two large aftershocks (M > 7) on March 11 (A1 and A2 in d.). (b) The Mw 9 earthquake and its aftershocks: for 1-day (solid black circles) and for the period up to t_{aft} = 100 days (gray shaded circles). Both $\eta_l(100)$ and $\eta_h(100)$ are less than 1.5 that are similar to those of a megathrust event in Alaska. (Aftershock area expansion pattern observed for the 2011 Tohoku-Oki.) (c) Illustration of plate coupling for NE Japan that is characterized by sparsely distributed small asperities, and considered weak. The aftershock area at a small t_{aft} (~1 day) is identified as an asperity. Aftershock areas expand into the surrounding areas significantly at a large t_{aft} (≥100 days), often overlapping that of an adjacent major event. A typical large source rupture has a characteristic time τ of 10 to 15 s. (d) A fault zone is characterized with a uniform, large asperity and the interplate coupling is considered strong such as in the Alaskan subduction zone. The source-process time τ of the 1964 Alaska earthquake (Mw 9.2) was ~180 s, and the aftershock area does not expand much at a large t_{aft}.

large tsunamis. However, for evaluating tsunami hazards, the important issue is not the overall size (moment) of the earthquake, but the possibility that large slip can occur on the shallow region near the trench. Past M 8 class earthquakes in 1896 and 1933 in the Tohoku-Oki region also produced tsunamis of 20 to 30 m (Kanamori, 1971; Tanioka and Satake, 1996) nearly as high as the 2011 event.

3.5. Foreshock and aftershock patterns and triggered events

The rupture pattern of the 2011 Tohoku-Oki earthquake sequence that started with a Mw 7.3 foreshock which is similar in size to previous events in this region (Fig. 9; Tajima and Kennett, 2012). The expansion of the 2-day aftershock area of the March 9 foreshock stopped at the impending March 11 mainshock epicenter that took place at the western edge of the zone (Fig. 9a). This expansion pattern which could have triggered the mainshock can be interpreted in several ways, such as diffusional propagation of the after-slip of the foreshock (Ando and Imanishi, 2011), propagation of slow slip prior to the March 9 event (Kato et al., 2012) or episodic transient slow slip events over a longer period (Ito et al., in press). The March 11 main event ruptured a broad region in τ ~ 150 s and was followed within a few hours by two large thrust aftershocks (Mw 7.9, Mw 7.1) and an outer-rise normal-faulting event (Mw 7.7) near the southern end of the 1933 rupture zone (Lay et al., 2011b). However, it is notable that the aftershock area did not show much expansion over time as compared with the 1-day area despite the numerous aftershocks. Instead areas of relatively low slip during the main rupture are progressively filled in by the aftershocks, particularly bigger aftershocks fit in the larger 'holes' in the main rupture slip distribution (Fig. 9b). (Here we consider the aftershock area to be closely associated with the main rupture zone, while the large events (M > 6) in Niigata and Shizuoka, which occurred at distances of several hundred kilometers, and were apparently induced after March 11, are considered to be a separate type of triggering as discussed below). Unlike the previous

large earthquakes in this subduction zone, this expansion pattern is similar to that of asperity group 1 (see Section 2.3).

After the Mw 9 earthquake, numerous intraplate earthquake occurred beneath the outer slope of the Japan Trench including the large normal faulting aftershock (Mw 7.7) on March 11. Using data from ocean bottom seismic instruments, Obana et al. (2012) determined the locations and focal mechanisms of these events, and suggested that the stress regime at around 40 km depth in the Pacific plate was changed from compressional to tensional by the 2011 earthquake. They further suggest that the tensional stresses (which now extend to depths of about 40 km) may play an important role not only in the occurrence of large normal-faulting earthquakes, but also in hydration of the uppermost mantle of the incoming Pacific plate prior to the subduction.

Earthquakes that occur relatively far from the mainshock fault rupture can be explained as being induced by static and/or dynamic stress changes due to the mainshock. There were 6 M >5.0 earthquakes that occurred at distances of a few hundred kilometers during the 5 days following the mainshock. Also, 13 volcanoes in central and southwest Japan showed increased seismic activity. Miyazawa (2011) shows that early post-seismic events triggered by the 2011 Mw 9.0 Tohoku-Oki earthquake systematically propagated across southwestern Japan, associated with the strong seismic waves from the source. The propagation front traveled at 3.1 to 3.3 km/s and extended to a distance of 1350 km (Fig. 10), suggesting dynamic triggering. There were much fewer observations of triggered earthquakes in the northern direction, where dynamic stresses were smaller and did not exceed an apparent threshold of about 500 kPa in stress or 10^{-6} in strain.

Static stress changes closer to the source also contributed to triggered earthquakes (Hiratsuka and Sato, 2011; Sato et al., 2011; Toda et al., 2011a,b). Toda et al. (2011b) analyzed the post-seismic stress transfer from the mainshock to investigate a broad increase in seismicity rate for M≥2 earthquakes for distances up to 425 km from the location of large coseismic slip (≥15 m) on onshore Japan, parts of the Japan Sea and the Izu islands. They explored the possibility that the rate changes are the product of static Coulomb stress transfer to small faults, and suggested that seismicity can increase in the nominal stress shadow of a mainshock if small geometrically diverse active faults exist. Also, Yoshida et al. (2012) investigated the static stress fields for onshore areas of eastern Japan before and after the Tohoku-Oki by inverting focal mechanism data. They pointed out the high induced seismicity in Kanto–Chubu region can be due to stress changes from the 2011 mainshock, which are in the same direction as the background stresses.

4. Structural influences

The analyses as summarized above characterize the source of the 2011 Tohoku-Oki earthquake with a long-duration source process

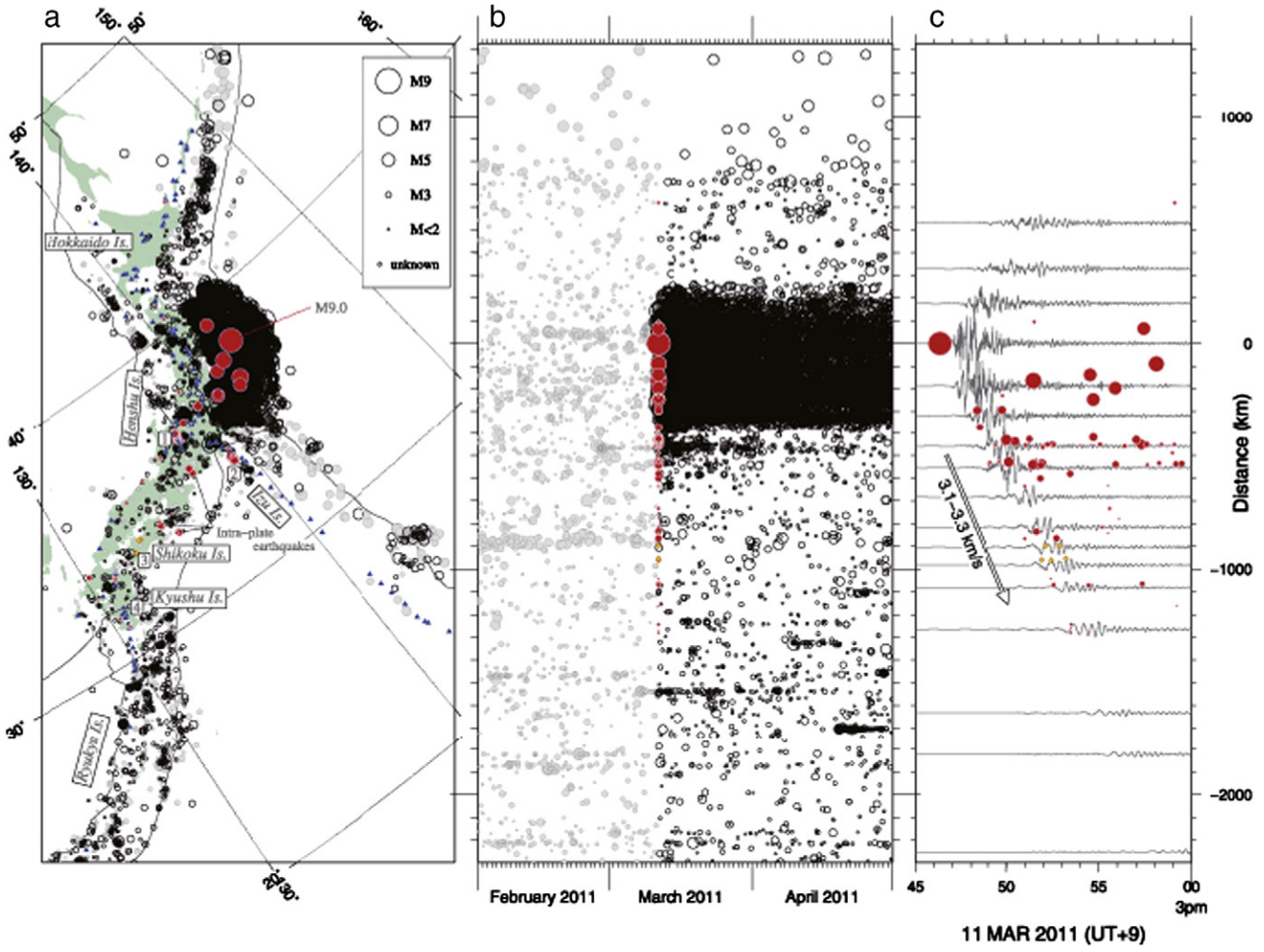

Fig. 10. Spatio-temporal distribution of events (M ≥2) shallower than 100 km over Japan before (shown with gray circles) and after (shown with black circles) the 2011 Tohoku-Oki earthquake (2011 February 1–April 30): (a) The epicenter distribution on a map view with early post-events detected in red and triggered non-volcanic tremor in yellow. (b) The temporal variation of seismicity projected with the vertical axis as a function of distance from the Tohoku-Oki earthquake epicenter. (c) The early stage post-seismicity events (shown with red) compared with some vertical component broadband seismograms (filtered at 0.01 to 1 Hz) at pertinent stations (Miyazawa, 2011).

(τ ~ 150 s) and a large rupture area of about 200 km × 500 km, which is distinctly separated into zones of high-frequency radiation down-dip and low-frequency radiation up-dip. What then produces the separation of rupture character within a single great earthquake? Significant clues are provided by the results of seismic tomography including those which were carried out before the event occurred, that point to substantial heterogeneity in the subducting slab and its environs. This heterogeneity appears to have contributed to the nature of the sub-events and their patterns of energy release during the recent great earthquake which had been ruptured in distinctive large earthquakes of M 7 to lower M 8 over the past few centuries.

4.1. Presence of heterogeneity in the subducting plate

There are a number of seismic tomography or 3D seismic wavespeed models for Japan. Matsubara and Obara (2011) produced a detailed P-wave tomography model for the region including the megathrust source area using arrival time and hypocentral data recorded by the NIED Hi-net and F-net. This model achieved a spatial resolution of 20 km horizontally and 10 km vertically near the Japan Trench, and reveals elevated P wavespeeds inside the subducting slab in the neighborhood of the epicentral area and two low-V_p zones within the subducting oceanic crust. The landward low-V_p zone with a large anomaly is consistent with the western edge of the coseismic slip zone of the 2011 Tohoku-Oki Earthquake. The asperities of the previously known Off-Miyagi and Off-Fukushima earthquakes with magnitudes around 7.0 are also located at the boundary of the landward low-*V* zone and the central high-*V* zone.

Zhao et al. (2011) relocated the 2011 mainshock and its foreshocks and aftershocks during the period of 2011 March 9–27 using a 3D regional model of P- and S-wavespeeds (Huang et al., 2011) and local P and S wave arrival times. The distribution of relocated hypocenters was then compared with a tomographic image in the region, which indicates that the rupture nucleations of the largest events (i.e., the March 9 foreshock of M 7.3, and three aftershocks with M > 7.0 on March 11), including the mainshock, were controlled by structural heterogeneities in the megathrust zone. Most of the large earthquakes are located in the high-velocity (high-*V*) patches or at the boundary between the low-*V* and high-*V* zones, with only a few situated in the low-*V* patches (Fig. 11; from Zhao et al., 2011). They pointed out very large variations in P wavespeed just above the upper surface of the subducting plate, and suggest that these wavespeed anomalies are related to frictional variations at the subduction interface.

Subducting seamounts are thought to increase the normal stress between subducting and overriding plates resulting in strong plate coupling. However, a recent seismic survey off the Ibaraki prefecture in the Japan Trench shows that a large seamount is being subducted near a region of repeating earthquakes of magnitude M ~ 7. Both observed seismicity and the pattern of rupture propagation during the 1982 M 7.0 event imply that interplate coupling is weak over the seamount (Mochizuki et al., 2008). A large rupture area with a small slip occurred in front of the seamount. Its northern bound could be determined by a trace of multiple subducted seamounts. Whereas a

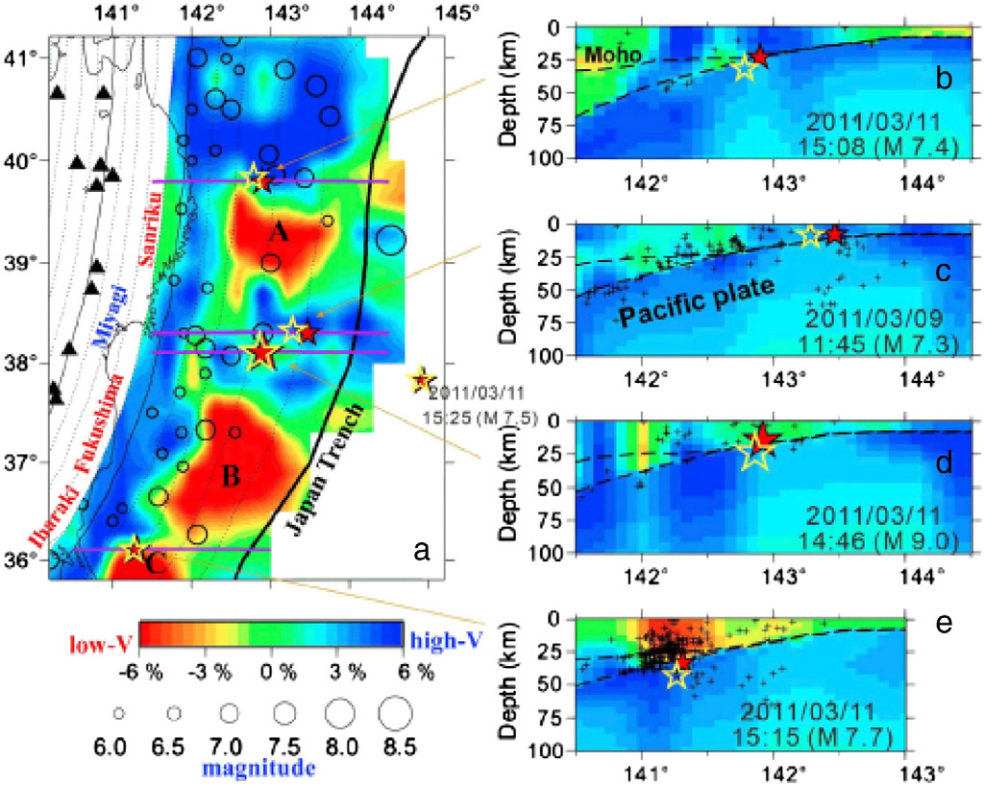

Fig. 11. P-wave tomographic image for the Tohoku-Oki region: (a) directly above the upper boundary of the subducting Pacific slab. Red and blue show low and high velocity anomalies, respectively. The velocity perturbation scale (in %) is shown at the bottom. Three low-velocity anomalies exist: (A) off Sanriku, (B) off Fukushima, and (C) off Ibaraki. The open circles denote the large earthquakes ($M_{JMA} \geq 6.0$) from 1900 to 2008, most of which were interplate earthquakes. East–west vertical cross sections of P-wave tomography passing through the epicenters of the 2011 Tohoku-Oki (d) mainshock, (c) foreshock, and (b, e) two aftershocks ($M_{JMA} > 7.0$). The relocated epicenters of the mainshock, the foreshock and the large aftershocks are plotted with red stars along with the epicenters listed in the JMA unified catalog (open yellow stars). The magnitude and origin time of these large earthquakes are shown in each of the cross sections. The two dashed lines in each cross section represent the Moho discontinuity and the upper boundary of the subducting Pacific plate. Cross symbols denote the relocated earthquakes during 2011 March 9–27 within a 10-km width to each profile (see Zhao et al., 2011).
Reproduced/modified by permission of American Geophysical Union.

subducted seamount itself may not define the rupture area, the rupture width may be influenced by that of the seamount.

4.2. Influence of heterogeneity on partitioning of rupture style

An alternative representation of the structural variations within the subducting slab is provided by Kennett et al. (2011), who consider the relative variations of shear-wave speed (β) and bulk-sound speed (ϕ, the wavespeed derived from bulk modulus alone) derived from the joint tomographic inversion of P and S wave arrivals (Gorbatov and Kennett, 2003). In the old subducting Pacific plate in the Japan area, shear wavespeed variations ($\delta\beta/\beta$) dominate variations in bulk-sound speed ($\delta\phi/\phi$) (the wavespeed associated with bulk-modulus alone). The variations in the wavespeed structure can be enhanced by examining a measure (R) (Kennett et al., 2011) of the relative variations in $\delta\phi/\phi$ and $\delta\beta/\beta$ with respect to the *ak135* reference model (Kennett et al., 1995).

$$R = \frac{1+\delta\beta/\beta}{1+\delta\phi/\phi} - 1, \tag{1}$$

where the seismic wavespeeds are given by $\beta^2 = G/\rho$, $\phi^2 = K_S/\rho$, in terms of the shear modulus G, bulk-modulus K_S, and density ρ. To first order, the measure R is simply the difference ($\delta\beta/\beta - \delta\phi/\phi$) and so enhances the subtle differences in the behavior of the shear and bulk moduli, since the density ρ is common to both wavespeeds.

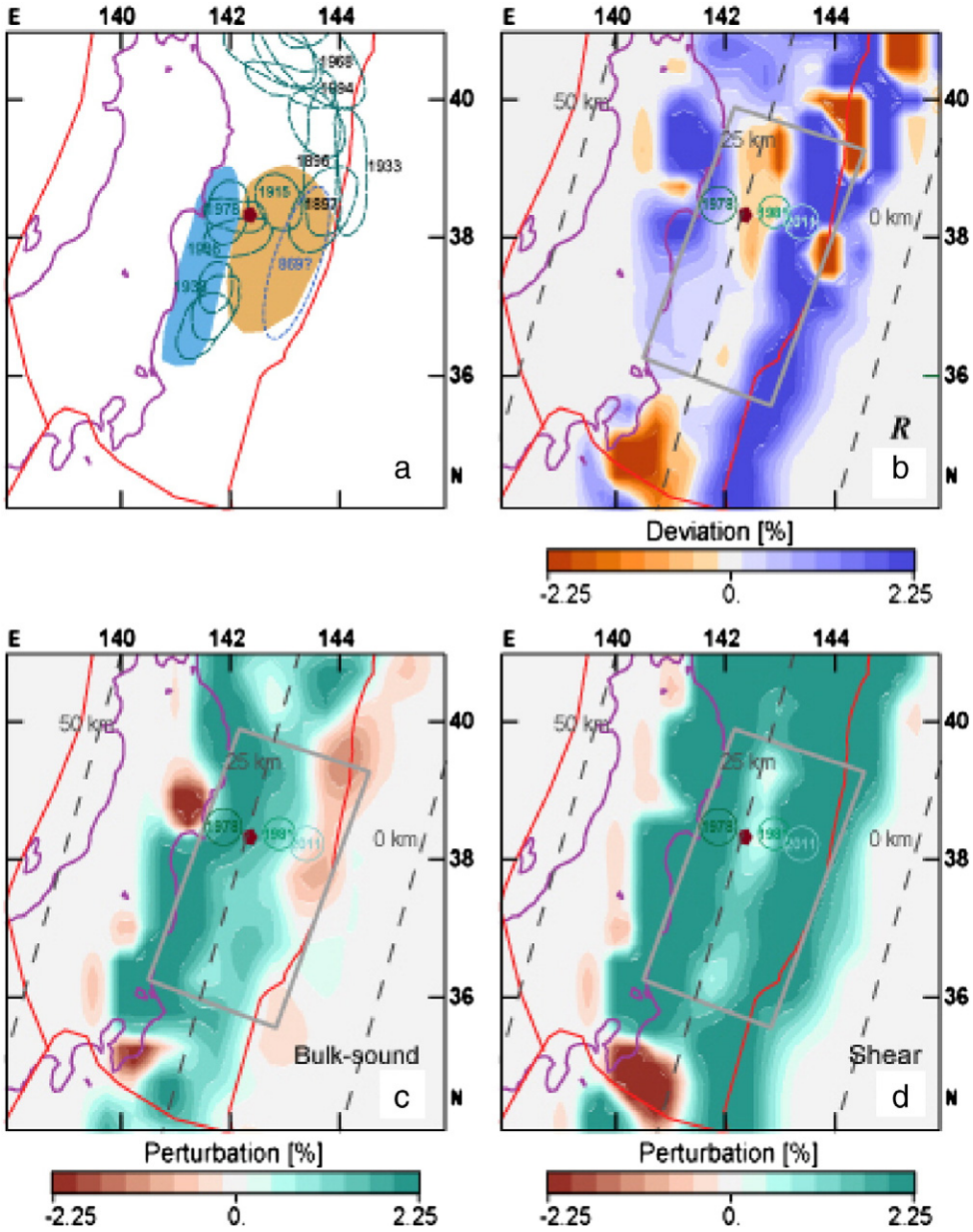

Fig. 12. Multiple images of the rupture area of the 2011 Tohoku-Oki event: (a) The locations of the zones of dominant high-frequency radiation (light blue) and dominant low-frequency energy radiations (buff) with the inferred rupture areas of past large earthquakes (green ellipses) superimposed. (b) The joint tomographic image for the ratio R (see the text) on an inclined plane with the depths indicated by dashed lines at 0, 25, and 50 km through the upper part of the subduction zone; reference point: 142°E, 38°N, 25 km depth, plane with dip azimuth 195°, dip angle 10°. The source area for the March 11 mainshock is outlined by a gray rectangle. The locations of the recent events (1978, 1981, 2011 March 9) are indicated together with the hypocenter of the March 11 event (red pentagon). (c) Bulk-sound speed tomographic image taken along the same inclined plane. (d) Shear wave speed tomographic image taken along the same inclined plane. Each of the tomographic quantities has been separately interpolated on to the inclined plane from the 3-D models, so there can be slight differences from direct construction of the fields on the plane (presented in Tajima and Kennett, 2012; reorganized from the joint tomography inversion model in Kennett et al., 2011; Gorbatov and Kennett, 2003).

Tomographic images are taken on a plane approximately coincident with the fault surface. *R* shows a distinct reduction to zero and slightly negative values (light orange) just up-dip of the mainshock hypocenter (Fig. 12b). The down-dip edge of this zone corresponds to the separation between the regions of dominant high-frequency radiation and dominant low-frequency radiation of the March 11 main rupture, and also the two major clusters of historical earthquake ruptures (Fig. 12a). In the lower two panels the images for $\delta\phi/\phi$ and $\delta\beta/\beta$ are shown separately (Fig. 12c, d). There is a significant gradient in $\delta\phi/\phi$, a slight negative anomaly near the trench, which then grades to stronger positive anomalies at depth. In contrast $\delta\beta/\beta$ is generally strongly positive with just a slight reduction at depths near 25 km, the hypocentral depth of the 2011 Tohoku-Oki earthquake (Fig. 12d). The zone of reduced *R* is largely associated with this reduction in $\delta\beta/\beta$ with the effects enhanced by the increase in $\delta\phi/\phi$, and appears to have a strong influence on plate coupling over the whole of the rupture area. The edges of the anomalous region we have delineated act as the initiation points for rupture process of the mainshock sequence as well as for 1978 (Mw 7.5) and 1981 (Mw 7.0) events, and these locations will be where the strongest contrasts exist in physical properties. The regional P wave tomography (Zhao et al., 2011) as described above indicates additional significant wavespeed variations above the slab interface that could affect the frictional properties at the plate boundary. Only a single event (M ~7.5) in 1915 appears to bridge between these two groupings (Kennett et al., 2011; Tajima and Kennett, 2012).

The anomalous structure has clearly been brought into the faulting region at the subduction interface with the subducting Pacific Plate, and may be associated with the Kashima facture zone (Nakanishi et al., 1992), which enters the Japan Trench just south of the rupture area of the 2011 event. Features with a similar orientation can be discerned on the incoming Pacific Plate. As the plate bends near the trench on entry to the subduction environment, there is ample opportunity for fluid ingress. Variations in structure in the plate are likely to lead to differences in the fluid regime once this portion of the plate moves to some depth and fluid begins to be expelled. The presence of fluid has a strong effect on shear wavespeed, and the structural anomalies in Fig. 12 may well represent the influence of fluids. Down-dip in a drier environment, slip can be sharp, but the presence of fluid will tend to lubricate motion and decrease inter-plate friction at shallower depths. The joint seismic tomography image (Gorbatov and Kennett, 2003), created prior to 2003, indicates significant clues to the impending March 2011 rupture process.

4.3. Stress transfer in heterogeneous structure

Ye et al. (2012) investigated the accumulated stress stage and transfer in a region of the megathrust fault, which is located near the northern termination of the Tohoku-Oki main rupture. This area was designated as the Sanriku-Oki low-seismicity region (SLSR), relative to adjacent regions, since it has relatively low levels of moderate-size ($M_j \geq 5.0$) earthquakes (see Fig. 13). The existence of such an SLSR was also pointed out by Kawakatsu and Seno (1983). The study by Ye et al. (2012) indicates that the southern portion of the SLSR appears to have had modest coseismic slip (<5 m) during the 2011 event and the postseismic convergence along the megathrust peaked in the SLSR with heightened aftershock activity including a Mw ~7.4 aftershock near its northeastern edge. The cause of the distinct nature of the frictional state on the SLSR relative to other parts of the megathrust is unclear. There is evidence for volumetric velocity heterogeneity in the vicinity of the 2011 Tohoku-Oki large slip zone, where relatively high V_p is observed (Zhao et al., 2011) and in the transition from large up-dip slip to lower down-dip slip (Kennett et al., 2011), where low shear velocity and low bulk sound velocity are observed. The latter study, along with that by Zhao et al. (2009), finds low velocities near the megathrust in the upper portion of the SLSR as well, with an increase in the ratio down-dip below the coastline. The presence of fluids could reduce the shear velocity and possibly the frictional strength in the aseismic region of the SLSR, but specific causes of the frictional behavior are not known.

The limited and localized occurrence of thrusting aftershocks suggests that most of the postseismic deformation in the SLSR is taking place aseismically. The average stress perturbation produced by the mainshock is evaluated using Coulomb 3 software for the southwestward

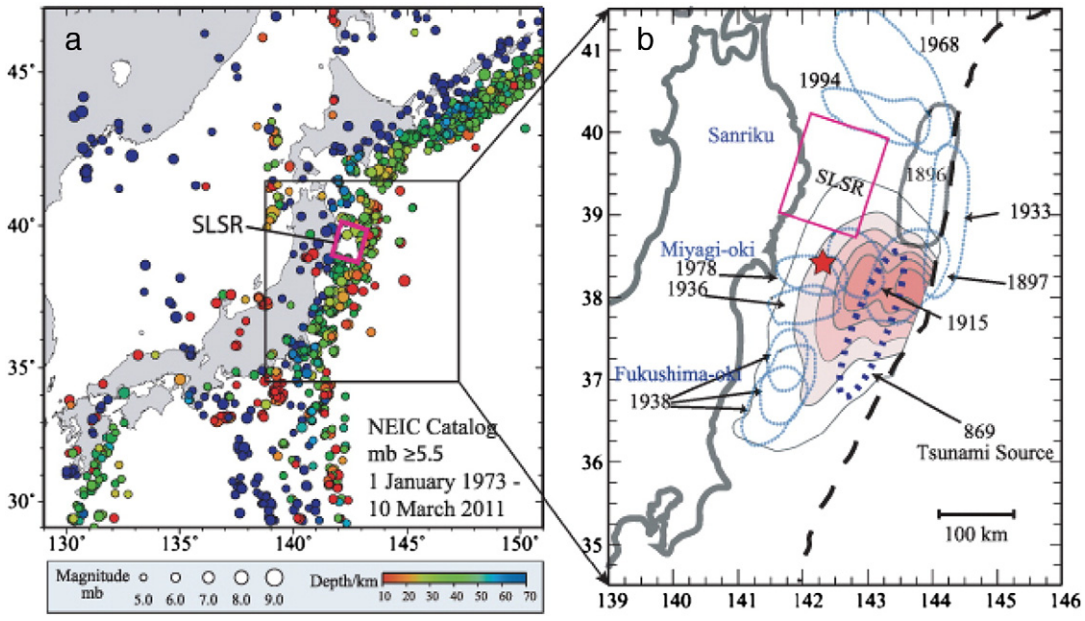

Fig. 13. (a) Seismicity from the NEIC catalog around Japan from 1973 to 2011 prior to the 2011 March 11 Tohoku-Oki earthquake with $m_b \geq 5.5$. Hypocentral depths are indicated by the color scale, and symbol size increases with seismic magnitude. The magenta rectangular indicates the region Sanriku low-seismicity region (SLSR). The black rectangle indicates the smaller region shown in (b). (b) Map showing the location of the SLSR, and schematic rupture zones of historic large earthquakes along the northeast Honshu coast (ERC) with blue thin dotted ellipses and the 1896 tsunami earthquake source area with a gray thick ellipse (Tanioka and Satake, 1996) up-dip of the SLSR, respectively. Slip contours of 1, 10, 20, 30, 40, and 50 m for the 2011 Tohoku-Oki rupture model of Yue and Lay (2011) are shown along with a red star for the USGS/NEIC epicentral location. The dark dotted ellipse indicates the approximate location of the 896 Jogan tsunami source region (Minoura et al., 2001). The dashed curve indicates the position of the trench (after Ye et al., 2012). Reproduced/modified by permission of American Geophysical Union.

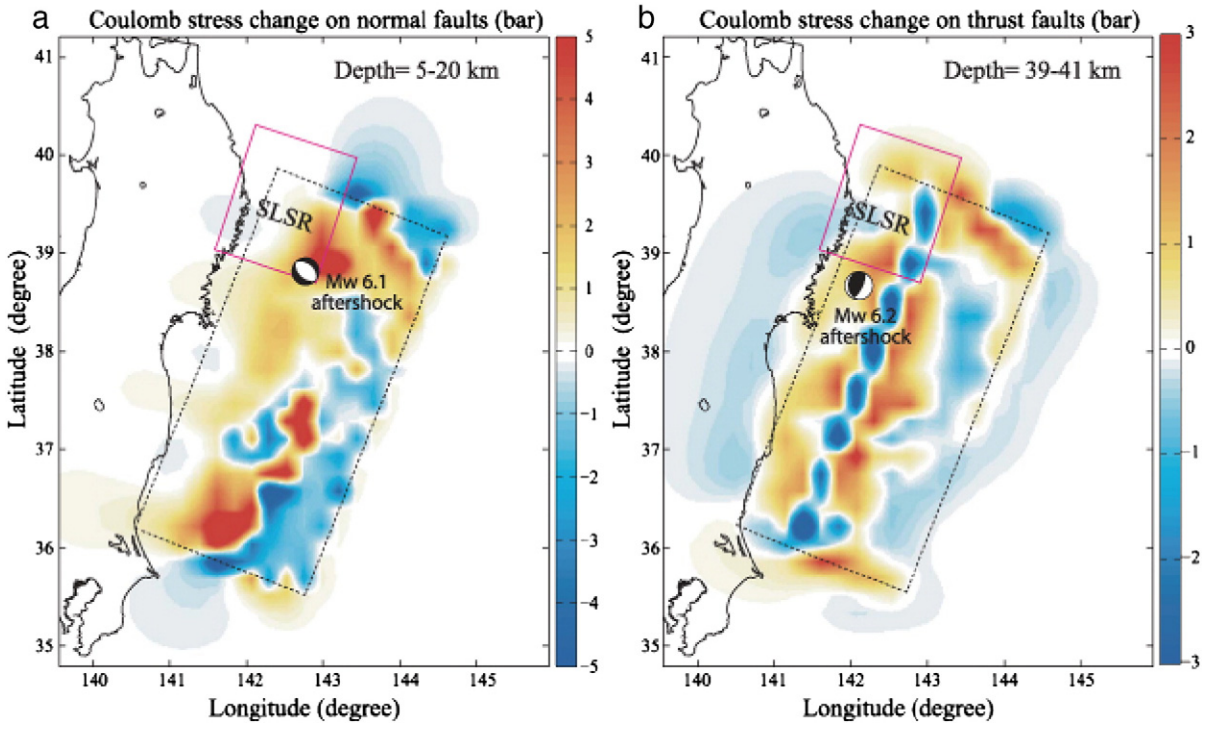

Fig. 14. Maps of Coulomb stress change predicted for the coseismic slip model from Yue and Lay (2011). (a) The Coulomb stress change averaged over the depth range 5–20 km for normal-faulting geometry given by the westward dipping plane of a Mw 6.1 aftershock located in the SLSR (2011 March 11, 20:11 UTC; strike = 140°, dip = 41°, rake = −76°; NIED CMT solution). (b) The Coulomb stress change over the depth range 39–41 km for a shallow-dipping thrust-faulting geometry given by a Mw 6.2 aftershock (March 25, 11:36:28.2 UTC; strike = 185°; dip = 26°; slip = 74°; NIED CMT solution), which is the largest aftershock modeled in Section 3.1 (from Ye et al., JGR 2012). Reproduced/modified by permission of American Geophysical Union.

dipping fault plane of a normal faulting geometry (5–20 km) given by a Mw 6.1 aftershock in the SLSR, and for a shallow-dipping thrust-faulting geometry of a Mw 6.2 aftershock located south of the SLSR. Results of Coulomb stress change for the coseismic slip model from Yue and Lay (2011) are shown in Fig. 14. However, Coulomb stress calculations generally provide only first-order guidance with respect to changes in the SLSR stress environment, as the ambient stresses are not known (Ye et al., 2012).

5. Discussion and conclusions

Since the last major seismic disaster caused by the 1995 Kobe earthquake (Mw 6.8), Japan has installed many advanced observation networks and a real-time Earthquake Early Warning system (EEW). These installations, in particular the real-time EEW system, aim to mitigate earthquake hazards by giving people and automated facilities time to take appropriate safety measures prior to the arrival of strong ground shaking and tsunamis. In this review we discussed on how rapidly the initiation of the megathrust earthquake was recognized using the real-time monitoring system and also summarized what limited the hazard reduction capability of the country with advanced infrastructure, i.e., the nature of the long-lasting complex source rupture process that broke through the broad region of heterogeneous plate coupling.

The real-time EEW system was able to quickly detect the onset of the large seismic rupture from the first arriving seismic signals, but failed to accurately estimate the total moment and large slip at shallower depths near the trench. The size of the earthquake was underestimated because of small amplitude in the initial phase and the long-duration of the entire rupture. Warnings of strong shaking were not provided to cellular telephones in the broader zone of areas affected by strong ground shaking in the Kanto region due to the underestimated moment, although information was sent out on televisions across the entire country. The large slip that occurred near the trench at about 50 s after the rupture initiation caused the tsunami catastrophe.

When the Mw 7.3 event occurred in the same subduction zone, off the coast of the Miyagi-prefecture on March 9, a spokesman in a TV news program warned that the aftershock activity could last with events of M > 6 for a week or so. This forecast was based on the assumption that the aftershock activity should decrease with time as represented by the modified Omori's law (Utsu, 1961). This formula does not account for the spatial extent of the affected area. The March 9 event turned to be a mere foreshock to the Mw 9 March 11 earthquake that released about 180 times as much energy as a Mw 7.5 event, and produced several dozens of aftershocks of M > 6.

Many specialists in Earth sciences and administrators in the government stated that a megathrust earthquake of this size had not been anticipated for this region, even though there were studies that had raised concerns about the significant deficit of tectonic stress release by previous large earthquakes. With the current level of preparedness for earthquake and tsunami hazards in Japan, the devastating tsunami catastrophe would not have been so serious had the rupture been limited to the size of a 'typical large earthquake of M ~7.5', since most barriers and gates designed to block tsunamis were 10 to 15 m high.

Numerous papers characterizing the Tohoku-Oki earthquake have demonstrated the significant advance in seismology and geophysical observations. These studies provide clues for improving the EEW system and the infrastructure for seismic and tsunami hazard reduction. The real-time system can be modified for progressive estimation of a rupture that evolves over a relatively long time into a very large event. Also, event discrimination needs to be improved for times of many aftershocks or swarm activity. During the Tohoku-Oki sequence, the system did not always work properly for aftershocks because arrival times from multiple events were not correctly associated.

Ohta et al. (2012) address the importance of real-time crustal deformation monitoring for rapid estimates of earthquake size (seismic moment or Mw). They developed an algorithm to identify permanent

displacements using real-time kinematic GPS (RTK-GPS) data. The method was tested using data from the 2011 Tohoku-Oki and was able to obtain a Mw 8.7 fault model, which is close to the actual Mw 9.0, within 5 min from the origin time. Once the fault mechanism has been estimated, tsunami waveforms can be synthesized quickly using pre-computed tsunami Green's functions. The calculated waveforms are in good agreement with the actual tsunami observations both in arrival time and wave height, which suggests that the RTK-GPS data can provide reliable estimate of the total moment and rapid tsunami forecasting to supplement the existing tsunami forecasting systems based on seismic observation.

Amplification effects of tsunamis were pointed out using satellite observations of sea level (Song et al., 2012). Model simulations, based on the GPS-derived earthquake source and constrained by measurements of seafloor motions near the hypocenter, confirm that the amplitudes are amplified by topographic refraction effects when tsunamis travel along ocean ridges and seamount chains. They point out that the effects of merging of multipathing tsunamis should be emphasized in mapping tsunami hazards and assessing risk levels at key coastal facilities.

There are many interpretations, models and arguments for the large scale rupture across the heterogeneous plate coupling. Kato and Yoshida (2011) conducted numerical modeling, in which a rate- and state-dependent frictional law was assumed along the interface of the subducting Pacific plate beneath northeastern Japan, to understand the mechanism of the Tohoku-Oki earthquake. They suggest that a strong asperity at shallow depths controls the occurrence cycle of great earthquakes. Further, Yoshida and Kato (2011) discussed effects of the pore pressure distribution along the same plate interface, and estimated nearly hydrostatic pore pressure (P_w) on the shallower part of the interface, and nearly lithostatic pressure on the deeper part of the interface. The effects of pore fluid pressure on the occurrence of interplate earthquakes have been addressed by many studies (see the summary by Seno, 2005, 2009). The analysis of the pore fluid pressure ratio λ ($= P_w/\sigma_n$; where σ_n is the normal stress) for major megathrust zones shows that this ratio for the region off the coast of Miyagi prefecture indicates potential for an M 9 class earthquake (Seno, personal communication).

High pore pressure within a fault zone is considered to be a possible cause for weakening plate boundaries (e.g., Rice, 1992). Based on the force balance in the forearc wedge, Seno (2009) estimated the pore fluid pressure ratio in the thrust zone off Miyagi as high as 0.960, which produces the average shear stress of 20 MPa. Hasegawa et al. (2011) and Yagi and Fukahata (2011a) argue that the Tohoku-Oki event completely released this amount of shear stress.

The occurrence of large interplate earthquakes may not be periodic if frictional stress is controlled by non-linear dynamic weakening of the fault. Along the Pacific coast of Hokkaido (northern most island of Japan), the recurrence intervals recorded in the tsunami deposits show considerable variation (100–800 years) (Nanayama et al., 2003; Sawai et al., 2009). Recently Seno (2012) disputed the characteristic recurrence interval of 100–150 years for great interplate earthquakes along the Nankai trough as the variation of recurrence interval has been in the range between 90 and 264 years (Ando, 1975).

There are also attempts to find clues that lead to such a gigantic rupture by looking at trends in various types of data. Heuret et al. (2012) compared relationships between upper plate strain, trench sediment thickness and maximal earthquake magnitude statistically and found that the combination of large trench fill ($\geq$1 km) and neutral strain in the upper plate strain explains the spatial patterns of giant earthquake occurrence to a statistically significant degree. The combination of these two factors is more correlated with giant earthquake occurrence than either factor alone. Less frequent giant earthquakes of lower magnitude are also possible at subduction zones with thinner trench fill and compressive upper plate strain. Extensional upper plate strain and trench fill <0.5 km appear to be unfavorable conditions, as giant earthquakes have not been observed in these geodynamical environments during the last 111 years.

An anomalous zone ($R<0$) identified in a joint tomography model (Gorbatov and Kennett, 2003; Kennett et al., 2011) is coincident with the mainshock initiation and the low-frequency energy radiation up-dip as well as the edges of the distinct rupture zones of the 1978, 1981, and 2011 March 9 earthquakes (see Fig. 12). The edges of these earthquake rupture zones are expected to have localized stress concentrations that were relieved during the aftershock area expansions. Expansions of the aftershock areas have occurred where the stress concentrations migrate beyond the rupture zones of the past large earthquakes, whereas the narrow area of the March 11 mainshock initiation remained intact until the tectonic stress level reached the maximum coupling strength, which is higher than in the surrounding areas. A conceptual model of progressive tectonic stress level can be drawn in relation to the heterogeneous plate coupling strength that accounts for the past individual seismic rupture zones (Tajima and Kennett, 2012). Whether the anomalies are due to the inherent physical properties or posterior features is still a subject to be investigated. Nonetheless the distribution of the heterogeneous shear strengths represents the effective plate coupling for interlocking the distinct source areas of prior earthquakes, and may be further investigated in relation to the pore fluid pressure ratio as described above.

The current practice of aftershock forecasts is based on the assumption that the aftershock activity decreases with time. The statistical features of aftershocks are described by a number of empirical laws concerning decreasing rates with time, such as the modified Omori's law (Utsu, 1961):

$$n(t) = \frac{K}{(c+t)^p} \tag{2}$$

where $n(t)$ is the rate of earthquake occurrence as a function of t after the main shock, K is the amplitude, and c is a constant. The index p typically falls in the range from 0.7 to 1.5. In this formula the aftershock activity (or frequency of occurrence) decreases by roughly the reciprocal of time when p is 1. The statistical features of foreshocks can also be described using a combination of the modified Omori's law and the Gutenberg–Richter relation (Jones, 1985). Seismicity rates in California and Japan show that there is a similar probability of about 5 to 10% that an earthquake will be followed within a few days by a larger earthquake in the immediate area (Jones, 1985; Smyth et al., 2011). Thus, the occurrence of the 2011 mainshock after the activity on March 9 is not unexpected. However, the designation of an earthquake as *foreshock*, *mainshock*, or *aftershock* is possible only after the sequence, primarily due to the uncertainty of the extent of the rupture propagation. This is a difficult part in earthquake prediction practice.

Recently Tiampo and Shcherbakov (2012) reviewed techniques which have been developed for seismicity-based earthquake forecasting. Comparison of the methods suggests that while smoothed seismicity models provide improved forecast capability over longer time periods, higher probability gain over shorter time periods is achieved with methods that integrate statistical techniques with knowledge of the physical process. In general, while both classes of seismicity-based forecasts are limited by the relatively short time period available for the instrumental catalog, significant advances have been made in our understanding of both the limitations and potential of seismicity-based earthquake forecasting. This recent progress serves to illuminate both the critical nature of the different temporal scales intrinsic to the earthquake process, and the importance of high quality seismic data for the accurate quantification of time-dependent earthquake hazard. The question "The Gutenberg–Richter or characteristic earthquake distribution, which is it?" (Wesnousky, 1994) has received the response "the statistical analysis supporting the characteristic model can be shown to be significantly deficient" and noted that accumulating

evidence calls into question the whole basis of the characteristic hypothesis, at least in the form it has been formulated and practiced (Kagan, 1996).

In summary the recent megathrust earthquake changed our understanding of seismic rupture, and stress propagation and migration at the plate boundary in the Tohoku region. What we had assumed for the impending scenario of seismic activity from the historical events of the past few centuries was a major underestimate of the maximum size event for this subduction zone. The 2011 Tohoku-Oki earthquake is a megathrust event which combined source areas that had remained distinct over the past few centuries. We reiterate that once an earthquake rupture initiates, it is currently difficult to determine how far it will propagate, and thus to what size it will grow. In a given subduction zone we have to be able to deal with events of large (and small) ruptures and subsequent tsunamis, which threaten human society. This review is intended to share information about the source rupture characteristics, plate boundary coupling strength and structures, as well as surface observations of deformations associated with the 2011 megathrust event. We also address issues that could contribute to hazard mitigation practices and forecasts of hypothetical future megathrust earthquakes in other subduction zones, such as those along the Nankai trough in Japan and Cascadia in North America.

Acknowledgments

We thank the Editor, Mian Liu, and two anonymous reviewers for their positive and constructive comments and suggestions. We are grateful to Tetsuzo Seno who provided with a number of useful suggestions and criticisms on the historical earthquakes and pore pressure arguments during the revision procedure. FT thanks Anke Friedrich for organizing the special session “Recent Megathrust Earthquakes and Tsunamis: Observations and Processes” at the GSA international conference, *Fragile Earth*, held in Munich, Germany for 4–7, September, 2011, and Heiner Igel for serving as the co-convener of the session. The special session led us to write this review article. We appreciate Tim Horscroft, Review Paper Coordinator for Earth Sciences Journals at Elsevier for giving us the opportunity to contribute this article to Tectonophysics. Yoshiko Yamanaka and Yoshihiro Ito kindly provided us with the original files for Figs. 2 and 7, respectively. We used the GMT software (Wessel and Smith, 1995) to draw maps.

References

Ammon, C.J., Lay, T., Kanamori, H., Cleveland, M., 2011. A rupture model of the 2011 off the Pacific coast of Tohoku Earthquake. Earth, Planets, and Space 63, 693–696. http://dx.doi.org/10.5047/eps.2011.05.015.

Ando, M., 1975. Source mechanisms and tectonic significance of historical earthquakes along the Nankai Trough, Japan. Tectonophysics 27, 119–140. http://dx.doi.org/10.1016/0040-1951(75)90102-X.

Ando, R., Imanishi, K., 2011. Possibility of Mw 9.0 mainshock triggered by diffusional propagation of after-slip from Mw 7.3 foreshock. Earth, Planets, and Space 63, 767–771. http://dx.doi.org/10.5047/eps.2011.05.016.

Duputel, Z., Rivera, L., Kanamori, H., Hayes, G.P., Hirshorn, B., Weinstein, S., 2011. Real-time W phase inversion during the 2011 off the Pacific coast of Tohoku Earthquake. Earth, Planets, and Space 63, 535–539. http://dx.doi.org/10.5047/eps.2011.05.032.

Fujii, Y., Satake, K., Sakai, S., Shinohara, M., Kanazawa, T., 2011. Tsunami source of the 2011 off the Pacific coast of Tohoku Earthquake. Earth, Planets, and Space 63, 815–820. http://dx.doi.org/10.5047/eps.2011.06.010.

Fujiwara, T., Kodaira, S., No, T., Kaiho, Y., Takahashi, N., Kaneda, Y., 2011. The 2011 Tohoku-Oki earthquake: displacement reaching the trench axis. Science 334, 1240.

Fukao, Y., 1979. Tsunami earthquakes and subduction processes near deep-sea trenches. Journal of Geophysical Research 84 (B5), 2303–2314. http://dx.doi.org/10.1029/JB084iB05p02303.

Furumura, T., Takemura, S., Noguchi, S., Takemoto, T., Maeda, T., Iwai, K., Padhy, S., 2011. Strong ground motions from the 2011 off-the-Pacific-Coast-of-Tohoku, Japan (Mw = 9.0) earthquake obtained from a dense nationwide seismic network. Landslides 8, 333–338. http://dx.doi.org/10.1007/s10346-011-0279-3.

Gorbatov, A., Kennett, B.L.N., 2003. Joint bulk-sound and shear tomography for Western Pacific subduction zones. Earth and Planetary Science Letters 210, 527–543.

Hara, T., 2011. Magnitude determination using duration of high frequency energy radiation and displacement amplitude: application to the 2011 off the Pacific coast of Tohoku Earthquake. Earth, Planets, and Space 63, 525–528. http://dx.doi.org/10.5047/eps.2011.05.014.

Hasegawa, A., Yoshida, K., Okada, T., 2011. Nearly complete stress drop in the 2011 Mw 9.0 off the Pacific coast of Tohoku Earthquake. Earth, Planets, and Space 63, 703–707. http://dx.doi.org/10.5047/eps.2011.06.007.

Hashimoto, C., Noda, A., Sagiya, T., Matsu'ura, M., 2009. Interplate seismogenic zones along the Kuril–Japan trench inferred from GPS data inversion. Nature Geoscience 2, 141–145. http://dx.doi.org/10.1038/NGEO421.

Hashimoto, C., Noda, A., Matsu'ura, M., 2012. The *Mw* 9.0 northeast Japan earthquake: total rupture of a basement asperity. Geophysical Journal International. http://dx.doi.org/10.1111/j.1365-246X.2011.05368.x.

Hayes, G.P., 2011. Rapid source characterization of the 03-11-2011 *Mw* 9.0 off the Pacific coast of Tohoku earthquake. Earth, Planets, and Space 63, 529–534. http://dx.doi.org/10.5047/eps.2011.05.012.

Hayes, G.P., Earle, P.S., Benz, H.M., Wald, D.J., Briggs, R.W., USGS/NEIC Earthquake Response Team, 2011. 88 hours: the U.S. Geological Survey National Earthquake Information Center response to the March 11, 2011 Mw 9.0 Tohoku earthquake. Seismological Research Letters 82 (4), 481–493.

Heuret, A., Conrad, C.P., Funiciello, F., Lallemand, S., Sandri, L., 2012. Relation between subduction megathrust earthquakes, trench sediment thickness and upper plate strain. Geophysical Research Letters 39, L05304. http://dx.doi.org/10.1029/2011GL05012.

Hiratsuka, S., Sato, T., 2011. Alteration of stress field brought about by the occurrence of the 2011 off the Pacific coast of Tohoku Earthquake (M_w 9.0). Earth, Planets, and Space 63, 681–685. http://dx.doi.org/10.5047/eps.2011.05.013.

Honda, R., Yukutake, Y., Ito, H., Harada, M., Aketagawa, T., Yoshida, A., Sakai, S., Nakagawa, S., Hirata, N., Obara, K., Kimura, H., 2011. A complex rupture image of the 2011 off the Pacific coast of Tohoku Earthquake revealed by the MeSO-net. Earth, Planets, and Space 63, 583–588.

Horiuchi, S., Negishi, H., Abe, K., Kaminuma, A., Fujinawa, Y., 2005. An automatic processing system for broadcasting earthquake alarms. Bulletin of the Seismological Society of America 95, 708–718.

Hoshiba, M., Iwakiri, K., 2011. Initial 30 seconds of the 2011 off the Pacific coast of Tohoku Earthquake (M_w 9.0) — amplitude and τ_c for magnitude estimation for Earthquake Early Warning. Earth, Planets, and Space 63, 553–557. http://dx.doi.org/10.5047/eps.2011.06.015.

Hoshiba, M., Kamigaichi, O., Saito, M., Tsukada, S., Hamada, N., 2008. Earthquake early warning starts nationwide in Japan. EOS, Transactions American Geophysical Union 89 (8), 73–74.

Hoshiba, M., Iwakiri, K., Hayashimoto, N., Shimoyama, T., Hirano, K., Yamada, Y., Ishigaki, Y., Kikuta, H., 2011. Outline of the 2011 off the Pacific coast of Tohoku Earthquake (M_w 9.0) — earthquake early warning and observed seismic intensity. Earth, Planets, and Space 63, 547–551. http://dx.doi.org/10.5047/eps.2011.05.031.

Huang, Z., Zhao, D., Wang, L., 2011. Seismic heterogeneity and anisotropy of the Honshu arc from the Japan Trench to the Japan Sea. Geophysical Journal International 184, 1428–1444. http://dx.doi.org/10.1111/j.1365-246X.2011.04934.x.

Ide, S., Baltay, A., Beroza, G.C., 2011. Shallow dynamic overshoot and energetic deep rupture in the 2011 Mw 9.0 Tohoku-Oki earthquake. Science 332, 1426–1429.

Igarashi, T., Matsuzawa, T., Hasegawa, A., 2003. Repeating earthquakes and interplate aseismic slip in the northeastern Japan subduction zone. Journal of Geophysical Research 108. http://dx.doi.org/10.1029/2002JB001920.

Iinuma, T., Ohzono, M., Ohta, Y., Miura, S., 2011. Coseismic slip distribution of the 2011 off the Pacific coast of Tohoku earthquake (M9.0) estimated based on GPS data — was the asperity in Miyagi-Oki ruptured? Earth, Planets, and Space 63, 643–648. http://dx.doi.org/10.5047/eps.2011.06.013.

Ishii, M., 2011. High-frequency rupture properties of the Mw 9.0 off the Pacific coast of Tohoku earthquake. Earth, Planets, and Space 63, 609–614. http://dx.doi.org/10.5047/eps.2011.07.009.

Ito, Y., Tsuji, T., Osada, Y., Kido, M., Inazu, D., Hayashi, Y., Tsushima, H., Hino, R., Fujimoto, H., 2011a. Frontal wedge deformation near the source region of the 2011 Tohoku-Oki earthquake. Geophysical Research Letters 38, L00G05. http://dx.doi.org/10.1029/2011GL048355.

Ito, T., Ozawa, K., Watanabe, T., Sagiya, T., 2011b. Slip distribution of the 2011 off the Pacific coast of Tohoku Earthquake inferred from geodetic data. Earth, Planets, and Space 63, 627–630. http://dx.doi.org/10.5047/eps.2011.06.023.

Ito, Y., Hino, R., Kido, M., Fujimoto, H., Osada, Y., Inazu, D., Ohta, Y., IInuma, T., Ohzono, M., Miura, S., Mishina, M., Suzuki, K., Tsuji, T., Ashi, J., in press. Episodic slow slip events in the Japan subduction zone before the 2011 Tohoku-Oki earthquake. Tectonophysics. http://dx.doi.org/10.1016/j.tecto.2012.08.022.

Jones, L.M., 1985. Foreshocks and time-dependent earthquake hazard assessment in southern California. Bulletin of the Seismological Society of America 84, 892–899.

Kagan, Y.Y., 1996. Comment on “The Gutenberg–Richter or characteristic earthquake distribution, which is it?” by Steven G. Wesnousky. Bulletin of the Seismological Society of America 86, 274–285.

Kanamori, H., 1971. Seismological evidence for a lithospheric normal faulting — the Sanriku earthquake of 1933. Physics of the Earth and Planetary Interiors 4, 289–300.

Kanamori, H., 1972. Mechanism of tsunami earthquakes. Physics of the Earth and Planetary Interiors 6, 346–359.

Kanamori, H., 1977. Seismic and aseismic slip along subduction zones and their tectonic implications, Island Arcs Deep Sea Trenches and Back-Arc Basins. In: Talwan, M., Pitman III (Eds.), Maurice Ewing Series, 1, pp. 163–174.

Kanamori, H., Miyazawa, M., Mori, J., 2006. Investigation of the earthquake sequence off Miyagi prefecture with historical seismograms. Earth, Planets, and Space 58, 1533–1541.

Kato, N., Yoshida, S., 2011. A shallow strong patch model for the 2011 great Tohoku-Oki earthquake: a numerical simulation. Geophysical Research Letters 38, L00G04. http://dx.doi.org/10.1029/2011GL048565.

Kato, A., Obara, K., Igarashi, T., Tsuruoka, H., Nakagawa, S., Hirata, N., 2012. Propagation of slow slip leading up to the 2011 M_w9.0 Tohoku-Oki earthquake. Science 335, 705–708. http://dx.doi.org/10.1126/science.1215141.

Kawakatsu, H., Seno, T., 1983. Triple seismic zone and the regional variation of seismicity along the northern Honshu arc. Journal of Geophysical Research 88, 4215–4230.

Kayanne, H., Ikeda, Y., Echigo, T., Shishikura, M., Kamataki, T., Satake, K., Malik, J.N., Basir, S.R., Chakrabortty, G.K., Ghosh Roy, A.K., 2007. Coseismic and postseismic creep in the Andaman Islands associated with the 2004 Sumatra–Andaman earthquake. Geophysical Research Letters 34. http://dx.doi.org/10.1029/2006GL028200.

Kennett, B.L.N., Engdahl, E.R., Buland, R., 1995. Constraints on seismic velocities in the Earth from travel times. Geophysical Journal International 122, 108–124.

Kennett, B.L.N., Gorbatov, A., Kiser, E., 2011. Structural controls on the Mw 9.0 2011 Offshore Tohoku earthquake. Earth and Planetary Science Letters 310, 462–467.

Kido, M., Osada, Y., Fujimoto, H., Hino, R., Ito, Y., 2011. Trench-normal variation in observed seafloor displacements associated with the 2011 Tohoku-Oki earthquake. Geophysical Research Letters 38, L24303. http://dx.doi.org/10.1029/2011GL050057.

Kiser, E., Ishii, M., 2012. The March 11, 2011 Tohoku-Oki earthquake and cascading failure of the plate interface. Geophysical Research Letters 39, L00G25. http://dx.doi.org/10.1029/2012GL051170.

Koketsu, K., Yokota, Y., Nishimura, N., Yagi, Y., Miyazaki, N., Satake, K., Fujii, Y., Miyake, H., Sakai, S., Yamanaka, Y., Okada, T., 2011. A unified source model for the 2011 Tohoku earthquake. Earth and Planetary Science Letters 310, 480–487. http://dx.doi.org/10.1016/j.epsl.2011.09.009.

Koper, K.D., Hutko, A.R., Lay, T., Ammon, C.J., Kanamori, H., 2011a. Frequency dependent rupture process of the 2011 *Mw* 9.0 Tohoku Earthquake: comparison of short-period P wave back-projection images and broadband seismic rupture models. Earth, Planets, and Space 63, 599–602. http://dx.doi.org/10.5047/eps.2011.05.026.

Koper, K.D., Hutko, A.R., Lay, T., 2011b. Along-dip variation of teleseismic short period radiation from the 11 March 2011 Tohoku Earthquake (Mw 9.0). Geophysical Research Letters 38, L21309. http://dx.doi.org/10.1029/2011GL049689.

Kurahashi, S., Irikura, K., 2011. Source model for generating strong ground motions during the 2011 off the Pacific coast of Tohoku Earthquake. Earth, Planets, and Space 63, 571–576. http://dx.doi.org/10.5047/eps.2011.06.044.

Lay, T., Kanamori, H., 1981. An asperity model of large earthquake sequences. Earthquake Prediction — An International Review: Maurice Ewing Series, 4, pp. 579–592.

Lay, T., Kanamori, H., 2011. Insights from the great 2011 Japan earthquake. Physics Today 64, 33–39.

Lay, T., Kanamori, H., Ruff, L., 1982. The asperity model and the nature of large subduction zone earthquakes. Earthquake Prediction Research, 1. Terrapub, pp. 3–71.

Lay, T., Ammon, C.J., Kanamori, H., Xue, L., Kim, M.J., 2011a. Possible large near trench slip during the 2011 Mw 9.0 off the Pacific coast of Tohoku earthquake. Earth, Planets, and Space 63, 687–692. http://dx.doi.org/10.5047/eps.2011.05.033.

Lay, T., Ammon, C.J., Kanamori, H., Kim, M.J., Xue, L., 2011b. Outer trench-slope faulting and the 2011 M_w 9.0 off the Pacific coast of Tohoku Earthquake. Earth, Planets, and Space 63, 713–718. http://dx.doi.org/10.5047/eps.2011.05.006.

Lee, S.-J., Huang, B.-S., Ando, M., Chiu, H.-C., Wang, J.-H., 2011. Evidence of large scale repeating slip during the 2011 Tohoku-Oki earthquake. Geophysical Research Letters 38, L19306. http://dx.doi.org/10.1029/2011GL049580.

Loveless, J.P., Meade, B.J., 2010. Geodetic imaging of plate motions, slip rates, and partitioning of deformation in Japan. Journal of Geophysical Research 115, B02410. http://dx.doi.org/10.1029/2008JB006248.

Maeda, T., Furumura, T., Sakai, S., Shinohara, M., 2011. Significant tsunami observed at ocean-bottom pressure gauges during the 2011 off the Pacific coast of Tohoku earthquake. Earth, Planets, and Space 63, 803–808. http://dx.doi.org/10.5047/eps.2011.06.00.

Matsubara, M., Obara, K., 2011. The 2011 off the Pacific coast of Tohoku Earthquake related to a strong velocity gradient within the Pacific plate. Earth, Planets, and Space 63, 663–667. http://dx.doi.org/10.5047/eps.2011.05.018.

Matsuzawa, T., Igarashi, T., Hasegawa, A., 2002. Characteristic small-earthquake sequence off Sanriku, northeastern Honshu, Japan. Geophysical Research Letters 29. http://dx.doi.org/10.1029/2001GL014632.

Matsuzawa, T., Uchida, N., Igarashi, T., Okada, T., Hasegawa, A., 2004. Repeating earthquakes and quasi-static slip on the plate boundary east off northern Honshu, Japan. Earth, Planets, and Space 56, 803–811.

Meng, L., Inbal, A., Ampuero, J.P., 2011. A window into the complexity of the dynamic rupture of the 2011 Mw 9 Tohoku-Oki earthquake. Geophysical Research Letters 38, L00G07. http://dx.doi.org/10.1029/2011GL048118.

Minoura, K., Imamura, F., Sugawara, D., Kono, Y., Iwashita, T., 2001. The 869 Jogan tsunami deposit and recurrence interval of large-scale tsunami on the Pacific coast of northeast Japan. Journal of Natural Disaster Science 23, 83–88.

Miyazaki, S., McGuire, J.J., Segall, P., 2011. Seismic and aseismic fault slip before and during the 2011 off the Pacific coast of Tohoku Earthquake. Earth, Planets, and Space 63, 637–642. http://dx.doi.org/10.5047/eps.2011.07.001.

Miyazawa, M., 2011. Propagation of an earthquake triggering front from the 2011 Tohoku-Oki earthquake. Geophysical Research Letters 38, L23307. http://dx.doi.org/10.1029/2011 GL049795.

Mochizuki, K., Yamada, T., Shinohara, M., Yamanaka, Y., Kanazawa, T., 2008. Weak interplate coupling by seamounts and repeating M 7 earthquakes. Science 321, 1194–1197. http://dx.doi.org/10.1126/science.1160250.

Nakahara, H., Sato, H., Nishimura, T., Fujiwara, H., 2011. Direct observation of rupture propagation during the 2011 off the Pacific coast of Tohoku Earthquake (M_w 9.0) using a small seismic array. Earth, Planets, and Space 63, 589–594. http://dx.doi.org/10.5047/eps.2011.06.002.

Nakanishi, M., Tamaki, K., Kobayashi, K., 1992. Magnetic anomaly lineations from Late Jurassic to Early Cretaceous in the west-central Pacific Ocean. Geophysical Journal International 109, 701–719.

Nanayama, F., Satake, K., Furukawa, R., Shimokawa, K., Atwater, B.F., Shigeno, K., Yamaki, S., 2003. Unusually large earthquakes inferred from tsunami deposits along the Kuril trench. Nature 424, 660–663.

Nettles, M., Ekström, G., Koss, H.C., 2011. Centroid–moment–tensor analysis of the 2011 off the Pacific coast of Tohoku Earthquake and its larger foreshocks and aftershocks. Earth, Planets, and Space 63, 519–523. http://dx.doi.org/10.5047/eps.2011.06.009.

Nishimura, T., 2000. Spatiotemporal change of interpolate coupling in northeastern Japan inferred from GPS data, (in Japanese), Ds. Thesis, Tohoku Univ., Sendai, Japan. 123pp.

Nishimura, T., Miura, S., Tachibana, K., Hashimoto, K., Toshiya Sato, T., Hori, S., Murakami, E., Toshio Kono, T., 2000. Distribution of seismic coupling on the subducting plate boundary in northeastern Japan inferred from GPS observations. Tectonophysics 323, 217–238.

Nishimura, T., Hirasawa, T., Miyazaki, S., Sagiya, T., Tada, T., Miura, S., Tanaka, K., 2004. Temporal change of interplate coupling in northeastern Japan during 1995–2002 estimated from continuous GPS observations. Geophysical Journal International 157, 901–916. http://dx.doi.org/10.1111/j.1365-246X.2004.02159.x.

Nishimura, T., Munekane, H., Yarai, H., 2011. The 2011 off the Pacific coast of Tohoku Earthquake and its aftershocks observed by GEONET. Earth, Planets, and Space 63, 631–636. http://dx.doi.org/10.5047/eps.2011.06.025.

Obana, K., Fujie, G., Takahashi, T., Yamamoto, Y., Nakamura, Y., Kodaira, S., Takahashi, N., Kaneda, Y., Shinohara, M., 2012. Normal-faulting earthquakes beneath the outer slope of the Japan Trench after the 2011 Tohoku earthquake: implications for the stress regime in the incoming Pacific plate. Geophysical Research Letters 39, L00G24. http://dx.doi.org/10.1029/2011GL050399.

Ohta, Y., Kobayashi, T., Tsushima, H., Miura, S., Hino, R., Takasu, T., Fujimoto, H., Iinuma, T., Tachibana, K., Demachi, T., Sato, T., Ohzono, M., Umino, N., 2012. Quasi real-time fault model estimation for near-field tsunami forecasting based on RTK-GPS analysis: application to the 2011 Tohoku-Oki earthquake (Mw 9.0). Journal of Geophysical Research 117, B02311. http://dx.doi.org/10.1029/2011JB008750.

Okada, Y., Kasahara, K., Hori, S., Obara, K., Sekiguchi, S., Fujiwara, H., Yamamoto, A., 2004. Recent progress of seismic observation networks in Japan: Hi-net, F-net, K-NET and KiK-net. Earth, Planets, and Space 56, xv–xxviii.

Ozaki, T., 2011. Outline of the 2011 off the Pacific coast of Tohoku Earthquake (M_w 9.0) — tsunami warnings/advisories and observations. Earth, Planets, and Space 63, 827–830. http://dx.doi.org/10.5047/eps.2011.06.029.

Ozawa, S., Nishimura, T., Suito, H., Kobayahi, T., Tobita, M., Imakiire, T., 2011. Coseismic and postseismic slip of the 2011 magnitude-9 Tohoku-Oki earthquake. Nature 475, 373–376. http://dx.doi.org/10.1038/nature10227.

Polet, J., Thio, H.K., 2011. Rapid calculation of a Centroid Moment Tensor and waveheight predictions around the north Pacific for the 2011 off the Pacific coast of Tohoku Earthquake. Earth, Planets, and Space 63, 541–545. http://dx.doi.org/10.5047/eps.2011.05.005.

Pollitz, F., Bürgmann, R., Banerjee, P., 2011. Geodetic slip model of the 2011 M9.0 Tohoku earthquake. Geophysical Research Letters 38, L00G08. http://dx.doi.org/10.1029/2011GL048632.

Rice, J.R., 1992. Fault stress states, pore pressure distribution, and the weakness of the San Andreas Fault. In: Evans, B., Wong, T.-F. (Eds.), Fault Mechanics and Transport Properties in Rocks. Academic Press, pp. 475–503.

Roten, D., Miyake, H., Koketsu, K., 2012. A Rayleigh wave back-projection method applied to the 2011 Tohoku earthquake. Geophysical Research Letters 39, L02302. http://dx.doi.org/10.1029/2011GL050183.

Ruff, L., Kanamori, H., 1980. Seismicity and the subduction process. Physics of the Earth and Planetary Interiors 23, 240–252.

Ruff, L., Kanamori, H., 1983. The rupture process and asperity distribution of three great earthquakes from long-period diffracted P-waves. Physics of the Earth and Planetary Interiors 31, 202–230.

Saito, T., Ito, Y., Inazu, D., Hino, R., 2011. Tsunami source of the 2011 Tohoku-Oki earthquake, Japan: inversion analysis based on dispersive tsunami simulations. Geophysical Research Letters 38, L00G19. http://dx.doi.org/10.1029/2011GL049089.

Satake, K., Namegaya, Y., Yamaki, S., 2008. Numerical simulation of the AD 869 Jogan tsunami in Ishinomaki and Sendai plains. Annual Report on Active Fault and Paleoearthquake Researches 8, 71–89 (in Japanese with an English abstract).

Sato, M., Ishikawa, T., Ujihara, N., Yoshida, S., Fujita, M., Mochizuki, M., Asada, A., 2011. Displacement above the hypocenter of the 2011 Tohoku-Oki Earthquake. Science 332. http://dx.doi.org/10.1126/science.1207401.

Sawai, Y., et al., 2009. Aperiodic recurrence of geologically recorded tsunamis during the past 5500 years in eastern Hokkaido, Japan. Journal of Geophysical Research 114, B01319. http://dx.doi.org/10.1029/2007JB005503.

Seno, T., 1979. Intraplate seismicity in Tohoku and Hokkaido and large interpolate earthquakes: a possibility of a large interpolate earthquake off the southern Sanriku coast, northern Japan. J. Phys. Earth 27, 21–51.

Seno, T., 2005. Relations of interplate, intra-slab and intra-overriding-plate earthquakes in the case of Miyagi prefecture. Gekkan Chikyu 27, 62–66.

Seno, T., 2009. Determination of the pore fluid pressure ratio at seismogenic megathrusts in subduction zones: implications for strength of asperities and Andean-type mountain building. Journal of Geophysical Research 114, B05405. http://dx.doi.org/10.1029/2008JB005889.

Seno, T., 2012. Great earthquake along the Nankai trough — a new idea for their rupture mode and time series. Zisin 64, 97–116 (in Japanese with an English abstract).

Seno, T., Eguchi, T., 1983. Seismotectonics of the western Pacific region. In: Uyeda, S., Hilde, T.W.C. (Eds.), Tectonics of the Western Pacific–Indonesian Region. Geodynamics Series, 11. GSA/AGU, Washington D.C., pp. 5–40.

Seno, T., Shimazaki, K., Sommerville, P., Sudo, K., Eguchi, T., 1980. Rupture process of the Miyagi-Oki, Japan, earthquake of June 12, 1978. Physics of the Earth and Planetary Interiors 23, 39–61.
Shao, G., Li, X., Ji, C., Maeda, T., 2011. Focal mechanism and slip history of the 2011 Mw 9.1 off the Pacific coast of Tohoku Earthquake, constrained with teleseismic body and surface waves. Earth, Planets, and Space 63, 559–564. http://dx.doi.org/10.5047/eps.2011.06.028.
Shishikura, M., Sawai, Y., Okamura, Y., Komatsubara, J., Aung, T.-T., Ishiyama, T., Fujiwara, O., Fujino, S., 2007. Age and distribution of tsunami deposit in the Ishinomaki plain, northeastern Japan. Annual Report on Active Fault and Paleoearthquake Researches 7, 31–46.
Shishikura, M., Sawai, Y., Yukutani, Y., Okamura, Y., 2010. Simulation of the gigantic tsunami during Heian period — the 869 tsunami in Jogan era (in Japanese). Active Fault and Earthquake Research Center News, 16 . August, 1–16.
Simons, M., Minson, S.E., Sladen, A., Ortega, F., Jiang, J., Owen, S.E., Meng, L., Ampuero, J.-P., Wei, S., Chu, R., et al., 2011. The 2011 magnitude 9.0 Tohoku-Oki earthquake: mosaicking the megathrust from seconds to centuries. Science 332, 1421–1425.
Singh, S.C., Hananto, N., Mukti, M., Permana, H., Djajadihardja, Y., Harjono, H., 2011. Seismic images of the megathrust rupture during the 25th October 2010 Pagai earthquake, SW Sumatra: frontal rupture and large tsunami. Geophysical Research Letters 38, L16313. http://dx.doi.org/10.1029/2011GL048935.
Smyth, C., Mori, J., Yamada, M., 2011. Investigating the distributions of differences between mainshock and foreshock magnitude. Bulletin of the Seismological Society of America 101, 2626–2633. http://dx.doi.org/10.1785/0120110110.
Song, Y.T., Fukumori, I., Shum, C.K., Yi, Y., 2012. Merging tsunamis of the 2011 Tohoku-Oki earthquake detected over the open ocean. Geophysical Research Letters 39, L05606. http://dx.doi.org/10.1029/2011GL050767.
Suwa, Y., Miura, S., Hasegawa, A., Sato, T., Tachibana, K., 2006. Interplate coupling beneath NE Japan inferred from three-dimensional displacement field. Journal of Geophysical Research 111, B04402.
Suzuki, W., Aoi, S., Sekiguchi, H., Kunugi, T., 2011. Rupture process of the 2011 Tohoku-Oki mega-thrust earthquake (M9.0) inverted from strong-motion data. Geophysical Research Letters 38, L00G16. http://dx.doi.org/10.1029/2011GL049136.
Tajima, F., Kanamori, H., 1985a. Global survey of aftershock area expansion patterns. Physics of the Earth and Planetary Interiors 40, 77–134.
Tajima, F., Kanamori, H., 1985b. Aftershock area expansion and mechanical heterogeneity of fault zone within subduction zones. Geophysical Research Letters 12, 345–348.
Tajima, F., Kennett, B.L.N., 2012. Interlocking of heterogeneous plate coupling and aftershock area expansion pattern for the 2011 Tohoku-Oki Mw9 earthquake. Geophysical Research Letters 39, L05307. http://dx.doi.org/10.1029/2011GL050703.
Tanioka, Y., Satake, K., 1996. Fault parameters of the 1896 Sanriku tsunami earthquake estimated from tsunami numerical modeling. Geophysical Research Letters 23, 1549–1552. http://dx.doi.org/10.1029/96GL01479.
Tiampo, K.F., Shcherbakov, R., 2012. Seismicity-based earthquake forecasting techniques: ten years of progress. Tectonophysics 522–523, 89–121. http://dx.doi.org/10.1016/j.tecto.2011. 08.019.
Toda, S., Lin, J., Stein, R.S., 2011a. Using the 2011 M_w 9.0 off the Pacific coast of Tohoku Earthquake to test the Coulomb stress triggering hypothesis and to calculate faults brought closer to failure. Earth, Planets, and Space 63, 615–619. http://dx.doi.org/10.5047/eps.2011.05.010.
Toda, S., Stein, R.S., Lin, J., 2011b. Widespread seismicity excitation throughout central Japan following the 2011 M = 9.0 Tohoku earthquake and its interpretation by Coulomb stress transfer. Geophysical Research Letters 38, L00G03. http://dx.doi.org/10.1029/2011GL047834.
Tsai, V.C., Hayes, G.P., Duputel, Z., 2011. Constraints on the long-period moment-dip tradeoff for the Tohoku earthquake. Geophysical Research Letters 38, L00G17. http://dx.doi.org/10.1029/2011GL049129.
Tsuji, T., Ito, Y., Kido, M., Osada, Y., Fujimoto, H., Ashi, J., Kinoshita, M., Matsuoka, T., 2011. Potential tsunamigenic faults of the 2011 off the Pacific coast of Tohoku Earthquake. Earth, Planets, and Space 63, 831–834. http://dx.doi.org/10.5047/eps.2011.05.028.
Uchida, N., Hasegawa, A., Matsuzawa, T., Igarashi, T., 2004. Pre- and post-seismic slow slip on the plate boundary off Sanriku, NE Japan associated with three interplate earthquakes as estimated from small repeating earthquake data. Tectonophysics 385, 1–15. http://dx.doi.org/10.1016/j.tecto. 2004.04.015.
Usami, T., 1975. Descriptive Catalogue of Disaster Earthquakes in Japan. Univ. of Tokyo Press, Tokyo . 327 pp. (in Japanese).
Utsu, T., 1961. A statistical study on the occurrence of aftershocks. Geophysical Magazine 30, 521–605.
Utsu, T., 2004. Catalog of Damaging Earthquakes in the World (through 2002), the Dbase file distributed at the memorial party of Prof. Tokuji Utsu held in Tokyo. see http://iisee.kenken.go.jp/utsu/index_eng.html.
Wang, K., Hu, Y., 2006. Accretionary prisms in subduction earthquake cycles: the theory of dynamic Coulomb wedge. Journal of Geophysical Research 111, B06410. http://dx.doi.org/10.1029/2005JB004094.
Wang, D., Mori, J., 2011a. Rupture process of the 2011 off the Pacific coast of Tohoku earthquake (Mw 9.0) as imaged with back-projection of teleseismic P-waves. Earth, Planets, and Space 63, 603–607. http://dx.doi.org/10.5047/eps.2011.05.029.
Wang, D., Mori, J., 2011b. Frequency-dependent energy radiation and fault coupling for the 2010 Mw 8.8 Maule, Chile and 2011 Mw 9.0 Tohoku, Japan earthquakes. Geophysical Research Letters 38, L22308. http://dx.doi.org/10.1029/2011GL049652.
Wesnousky, S.G., 1994. The Gutenberg–Richter or characteristic earthquake distribution, which is it? Bulletin of the Seismological Society of America 84, 1940–1959.
Wessel, P., Smith, W.H.F., 1995. New version of the generic mapping tools released. EOS, Transactions American Geophysical Union 76, 329.
Yagi, Y., Fukahata, Y., 2011a. Rupture process of the 2011 Tohoku-Oki earthquake and absolute elastic strain release. Geophysical Research Letters 38, L19307. http://dx.doi.org/10.1029/2011GL048701.
Yagi, Y., Fukahata, Y., 2011b. Introduction of uncertainty of Green's function into waveform inversion for seismic source processes. Geophysical Journal International 186, 711–729. http://dx.doi.org/10.1111/j.1365-246X.2011.05043.x.
Yamanaka, Y., Kikuchi, M., 2004. Asperity map along the subduction zone in northeastern Japan inferred from regional seismic data. Journal of Geophysical Research 109, B07307. http://dx.doi.org/10.1029/2003JB002683.
Yamazaki, Y., Lay, T., Cheung, K.F., Yue, H., Kanamori, H., 2011. Modeling near-field tsunami observations to improve finite-fault slip models for the 11 March 2011 Tohoku earthquake. Geophysical Research Letters 38, L00G15. http://dx.doi.org/10.1029/2011GL049130.
Yao, H., Gerstoft, P., Shearer, P.M., Mecklenbräuker, C., 2011. Compressive sensing of the Tohoku-Oki Mw 9.0 earthquake: frequency-dependent rupture modes. Geophysical Research Letters 38, L20310. http://dx.doi.org/10.1029/2011GL049223.
Ye, L., Lay, T., Kanamori, H., 2012. The Sanriku-Oki low-seismicity region on the northern margin of the great 2011 Tohoku-Oki earthquake rupture. Journal of Geophysical Research 117, B02305. http://dx.doi.org/10.1029/2011JB008847.
Yokota, Y., Koketsu, K., Fujii, Y., Satake, K., Sakai, S., Shinohara, M., Kanazawa, T., 2011. Joint inversion of strong motion, teleseismic, geodetic, and tsunami datasets for the rupture process of the 2011 Tohoku earthquake. Geophysical Research Letters 38, L00G21. http://dx.doi.org/10.1029/2011GL050098.
Yoshida, S., Kato, N., 2011. Pore pressure distribution along plate interface that causes a shallow asperity of the 2011 great Tohoku-Oki earthquake. Geophysical Research Letters 38, L00G13. http://dx.doi.org/10.1029/2011GL048902.
Yoshida, Y., Ueno, H., Muto, D., Aoki, S., 2011a. Source process of the 2011 off the Pacific coast of Tohoku earthquake with the combination of teleseismic and strong motion data. Earth, Planets, and Space 63, 565–569. http://dx.doi.org/10.5047/eps.2011.05.011.
Yoshida, K., Miyakoshi, K., Irikura, K., 2011b. Source process of the 2011 off the Pacific coast of Tohoku Earthquake inferred from waveform inversion with long-period strong-motion records. Earth, Planets, and Space 63, 577–582. http://dx.doi.org/10.5047/eps.2011.06.050.
Yoshida, K., Hasegawa, A., Okada, T., Iinuma, T., Ito, Y., Asano, Y., 2012. Stress before and after the 2011 great Tohoku-Oki earthquake and induced earthquakes in inland areas of eastern Japan. Geophysical Research Letters 39, L03302. http://dx.doi.org/10.1029/2011GL049729.
Yue, H., Lay, T., 2011. Inversion of high-rate (1-sps) GPS data for rupture process of the 11 March 2011 Tohoku earthquake (Mw 9.1). Geophysical Research Letters 38, L00G09. http://dx.doi.org/10.1029/2011GL048700.
Zhang, H., Ge, Z., Ding, L., 2011. Three sub-events composing the 2011 off the Pacific coast of Tohoku Earthquake (Mw 9.0) inferred from rupture imaging by back projecting teleseismic P waves. Earth, Planets, and Space 63, 595–598. http://dx.doi.org/10.5047/eps.2011.06.021.
Zhao, D., Wang, Z., Umino, N., Hasegawa, A., 2009. Mapping the mantle wedge and interplate thrust zone of the northeast Japan arc. Tectonophysics 467, 89–106. http://dx.doi.org/10.1016/j.tecto.2008.12.017.
Zhao, D., Huang, Z., Umino, N., Hasegawa, A., Kanamori, H., 2011. Structural heterogeneity in the megathrust zone and mechanism of the 2011 Tohoku-Oki earthquake (Mw 9.0). Geophysical Research Letters 38, L17308. http://dx.doi.org/10.1029/2011GL048408.